17

Dynamic Tissue Perfusion Measurement – Basics and Applications

Thomas Scholbach
Chemnitz Clinics, Chemnitz
Germany

1. Introduction

1.1 Rationale

Perfusion is a fundamental prerequisite for all living tissues to meet their needs in terms of supply of oxygen, nutrients, hormones, messenger substances and other necessary dilutes. Dynamic Tissue Perfusion Measurement (DTPM) was developed to quantify the perfusion of tissues and organs by means of colour Doppler sonography. Perfusion is perceived as a certain amount of blood passing through a defined region of interest (ROI) in a certain time.

Colour Doppler sonography is universally used to visualize blood flow inside tissues. The velocity of moving red blood cells is depicted as coloured pixels on the background of uncoloured, black and white pixels, which describe parts of tissues without detectable blood flow. The colouration differs according to the velocity and direction of flow. A colour scale within each image shows the spectrum of reddish and bluish colours used to differentiate the direction (reddish hues describe flow which is reversely directed to bluish flow, in most cases the machine is set to depict flow towards the transducer in red). In both directions, lighter shades describe higher velocities than darker shades. A wall filter is used to exclude extremely low velocity signals from imaging, which mostly emanate from vessel wall vibrations and do not add to real blood flow. The colour scale or colour bar thus gives a visual clue to assign velocity signals from zero to a maximum value to certain vessels inside a tissue. At both ends of the colour scale, the maximum flow velocities for red and blue colour are depicted. These values are determined by the actual pulse repetition frequency and the applied ultrasound frequency. They correspond to the outermost hue on each side of the colour bar whereas the minimum flow is determined by the hue next to the black line (indicating the wall filter) separating blue and red hues from each other.

To calculate perfusion in a certain ROI two parameters must be known:

1. The flow velocity in all vessels within the ROI
2. The area of all vessel transsections in this ROI

Both parameters change during the heart cycle. A third prerequisite is thus to take into account these rhythmic changes and to refer them to their basic rhythm which is a full heart cycle.

DTPM makes use of the data offered by any colour Doppler machine, namely the real time depiction of rhythmically changing coloured pixels and the colour scale to gauge them. To achieve this each hue at the scale is assigned a specific velocity value. This value is calculated by the DTPM-software (PixelFlux, Chameleon-Software, Germany [1]) from a linear correlation of all colours from zero (the lower end of the scale) to the actual maximum value (which is depicted numerically at the outer end of the scale and corresponds to the lightest reddish and bluish shades of the scale). The PixelFlux-software also calculates the area of all coloured pixels inside the ROI. Thus, each coloured pixel is evaluated by assigning a specific velocity and area to it. This is possible only after calibrating the image.

Distance calibration is also done automatically by use of the DICOM data, which are delivered along with the image by the ultrasound machine. A so-called DICOM- header file accompanying each image contains non-visible data such as the type of the ultrasound machine, the transducer, the preset information, the patient data and the distance calibration among many other data.

The mean flow intensity (Q) inside a ROI with the area (A_{ROI}) is then automatically calculated by assigning each colour pixel a velocity (v) and area (A) value according to the following equation:

$$Q\ [cm/s] = v\ [cm/s]^* A\ [cm^2]/A_{ROI}\ [cm^2]$$

2. Standardized video acquisition

An indispensable precondition for reliable measurements is the use of comparable videos in terms of the imaging conditions applied to the investigated tissue. Only by keeping the fundamental circumstances of data acquisition constant, it is possible to compare the measurement results. Such parameters which need to be held constant are colour Doppler frequency and gain, type and software of the ultrasound machine, transducer type, persistence, wall filter, smoothing, type of the colour scale, preference for spatial versus time-resolution and others, depending on the actual configuration of the ultrasound machine. These parameters are summarized and stored as a certain preset of the machine and must be recalled at the beginning of an ultrasound investigation. This step is a widely used practice in order to maintain optimum imaging conditions also in examinations, where a measurement of image data is not a priori planned. The prepared preset is then re-instituted before recording videos for DTPM.

3. Setting the region of interest (ROI) and Doppler angle correction

The ROI is that area inside an ultrasound image, where tissue perfusion measurement is scheduled. The selection of the ROI depends on the type of tissue, structure of the organ and aim of the investigation. The following principles and physical restrictions should be kept in mind in defining the ROI.

In 2D-images, vessels are encoded in colour depending on the angle, which they have with the ultrasound wave. This propagation line of waves is oriented perpendicular to the transducer surface. The colouration represents the exact velocity value only in vessels running straight towards the transducer, i.e. parallel to the course of the sound wave propagation line. All other vessels are encoded with colour hues representing velocity

values (v) which are a product of the cosine of the Doppler angle (α) and the true velocity (v_t), according to the Doppler principle:

$$fd = 2* fo * v_t/c *\cos \alpha$$

with: fd: Doppler shift, fo: insonation frequency, c: sound velocity

This means that in many cases the tissue microvasculature colouration shows velocity values which are smaller than real. To overcome this, an angle correction for each vessel would be necessary. This cannot be done yet in two-dimensional images. With 3D imaging, such a correction is already feasible (see below in section "foetus"). In 2D images, thus an error occurs with DTPM, which must be kept constant to allow comparisons between investigations. This can be achieved under following circumstances:

1. A chaotic vessel architecture without predominant vessel diameters and Doppler angles (type tumour perfusion) (fig. 1)
2. A regular vessel architecture, which can be reliably retrieved (kidney type).

In the latter case, the orientation on anatomical landmarks offers a sufficient framework to find the vascular patterns, which are typical for a certain organ (fig. 2). An example how to choose relevant landmarks is given for the kidney below.

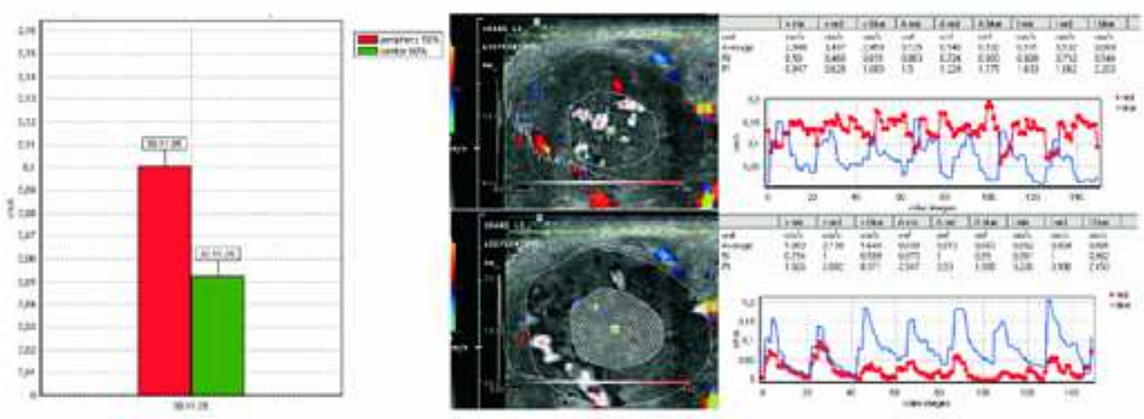

Fig. 1. Example of tumor perfusion measurement. Two concentric ROIs are separately investigated. The vessel architecture is irregular or chaotic (center). No specific prevailing vessel size or orientation can be stated. Left: comparisons of perfusion intensities in the periphery (red column) and the center (green column). Center: Display of the ROIs and false color maps with perfusion intensity curves. Right: time course of the relevant perfusion parameters (from [2])

In both cases, the inevitable error of impossible individual Doppler angle correction for each vessel is held constant. Comparisons of different examinations thus become possible.

For all these considerations, it is crucial to achieve comparable conditions for depicting the vessels in a certain ROI. In the kidney the ROI should be placed inside the outer cortex, in a layer stretching from the outer border of the medullary pyramids to the renal surface and laterally from the watershed of two neighbouring segments to the opposite watershed (see chapter: kidney). In the lymph node and thyroid lobes, a longitudinal section trough the

centre of the ovoid shaped organ should be used as definite transsection plane. In the bowel wall, a longitudinal cut perpendicular to the proximal wall is the best. Tumours should be cut centrally in two perpendicular planes.

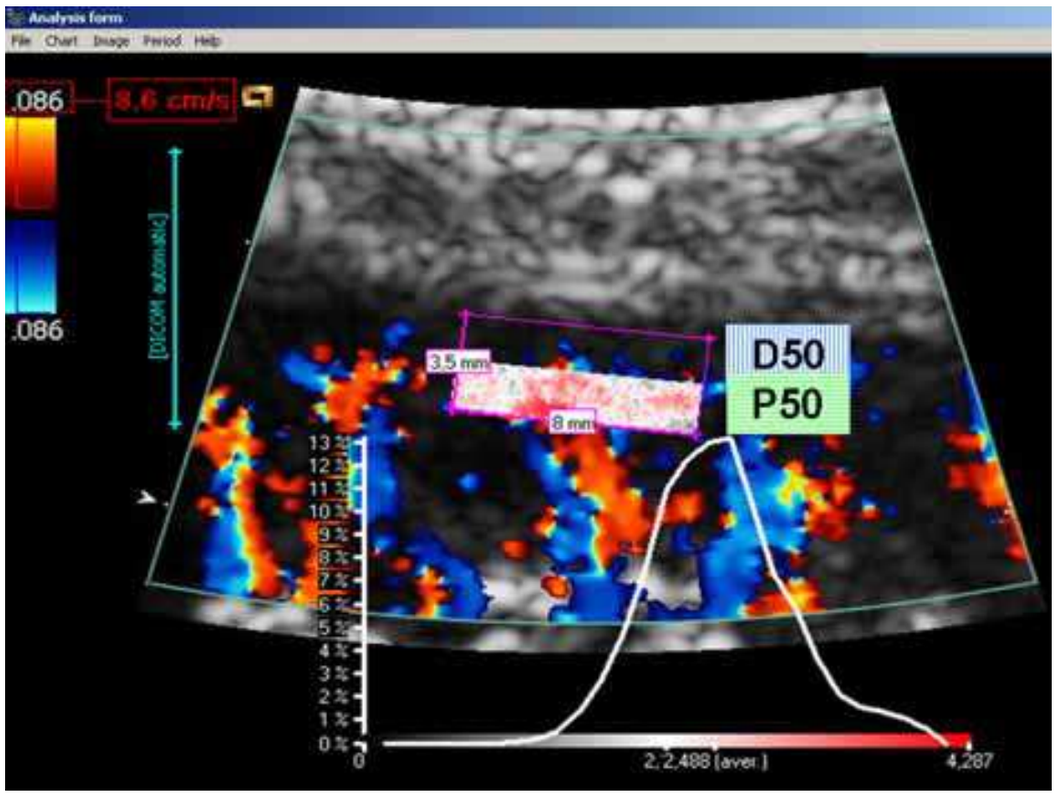

Fig. 2. Example for regular vessel architecture in a renal transplant – see also figure 3. The sub-ROIs are highlighted: P50 – proximal 50% of the outer cortex. D50- distal 50% of the outer cortex. False color map and distribution curve of perfusion intensities are displayed

4. Reading the results

Figure 3 gives an overview of the most important output features in a typical DTPM measurement. In DTPM all data are derived from the basic parameters mean flow velocity, mean perfused area and their change during the heart beat with reference to the entire ROI [2, 3]. In three-dimensional images, the spatial angle correction adds to the primary 2D measurement inside the horizontal plane.

In addition to mean perfusion intensity, calculation parameters are generated to describe the dynamics of perfusion. Examples are Tissue Resistance Index (TRI) and Tissue Pulsatility Index (TPI). TRI and TPI may refer to velocity, intensity and perfused area according to the following formulas:

TRI(velocity *or intensity or area*) = maximum mean velocity *or* intensity *or* area of the ROI during one heart cycle – minimum mean velocity *or intensity or area* of the ROI during one heart cycle divided by maximum mean velocity *or intensity or area* of the ROI during one heart cycle

TPI(velocity *or intensity or area*) = maximum mean velocity *or* intensity *or* area of the ROI during one heart cycle – minimum mean velocity *or intensity or area* of the ROI during one heart cycle divided by mean mean velocity *or intensity or area* of the ROI during one heart cycle

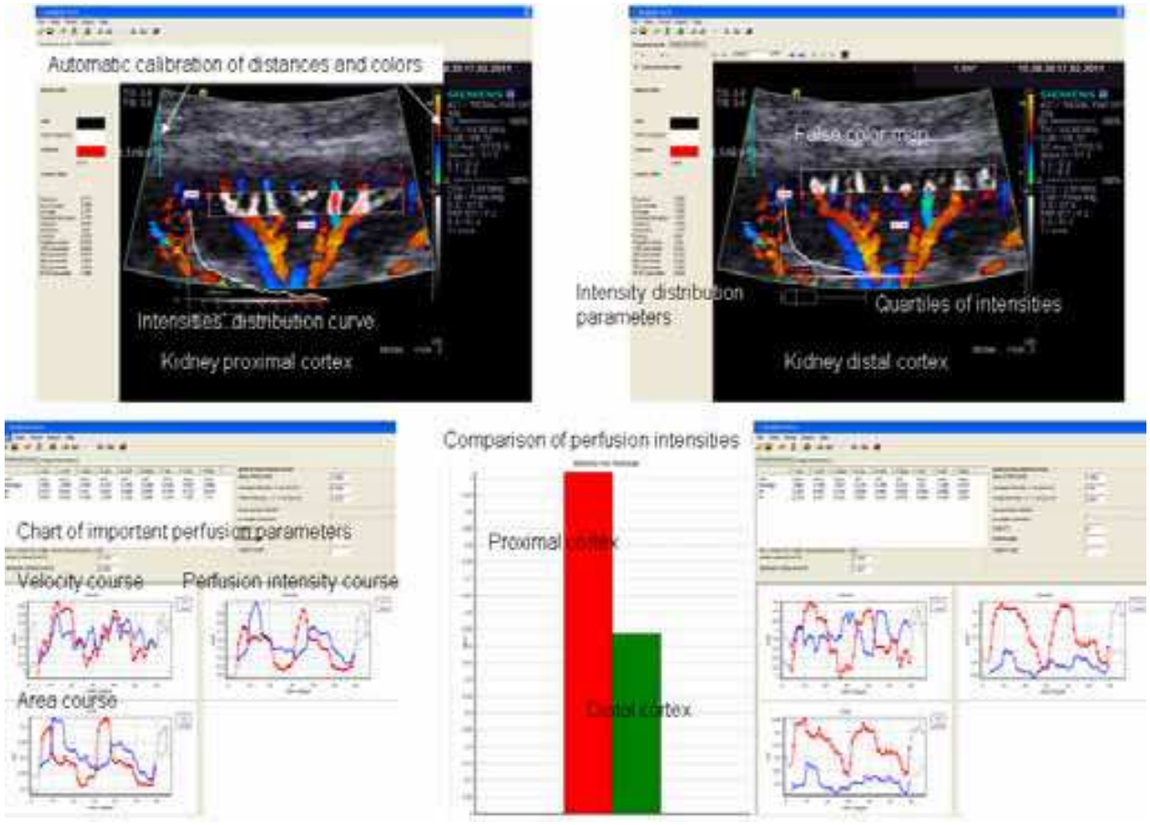

Fig. 3. Example of DTPM output. Overview of the most important output features of a DTPM measurement. Comparison of the proximal and distal cortical ROIs. False color maps (areas shaded in white, red and grey hues), perfusion intensities' distribution curves and additional parameters (upper line). Time curves of the basic perfusion parameters and perfusion intensities (below). Comparison of the overall perfusion intensities in both sub-ROIs (lower line center)

A dynamic perfusion map is generated to pinpoint the local perfusion in a sub-millimetre graded fashion numerically with false colours (fig. 2 and 13). Moreover, the distribution of perfusion intensities according to the whole spectrum of occurring intensities, which are assigned to one of 33 intensity classes, is calculated and diagrammatically displayed. Thus, tissues may be compared according to their content of stronger or weaker perfused areas and vessels (fig. 2, fig. 11). This allows insights into the microarchitecture of a tissue's vascular tree and its changes over time, which is helpful in chronic diseases and tumours. These intensity distribution curves are further described mathematically with the parameters kurtosis and skewness according to their bulging and asymmetry.

Altogether more than 50 parameters are calculated to describe the tissue perfusion numerically. The most important is perfusion intensity to give a general measure of tissue

perfusion. Very instructive too is the distribution curve, outlined below the false colour map (fig. 11). Here shifts within the microvessel population can be reviewed at a glance. This is further underlined with the distribution parameters skewness and kurtosis, which describe the shape of this curve numerically. Statistical comparison of microvessel arrangement thus becomes feasible, permitting the follow up of slight changes of an organ's chronic vascular changes, which begin in the periphery. Another important feature is the false colour map. This map stains the ROI according to the local perfusion intensities over the entire length of the colour Doppler sonographic video clip. The information added to the anatomical structures displayed by the ultrasound image can be helpful in differentiating parts of the tissue with respect to their vascular structures. The flow of the hepatic artery can be separated from the same coloured flow of the portal vein in this way, which might be welcome in the follow up of liver transplants. Another possible application might be the differentiation of local tissue disturbances, as caused by tumour infiltration or scarring or inflammation. To perform an automatic angle correction of all vessels 3D images are used. Here the spatial angel is calculated from both the angle in the frontal and in the sagittal plane. This angle then is applied to calculate true spatially angle corrected flow velocities and vessel diameters. Both are distorted in the original frontal view and can be corrected for 3D flow calculations in so doing. Another important feature is the use of predefined relational sub-ROIs to describe the blood flow on its way through the tissue. Gradients of perfusion can be used to quantify the dampening of perfusion in the depth of a vascular tree. This can be used to detect the very early loss of the tiniest vessels in a tissue, which are often the first to be damaged due to their small lumen. So a chronic pathological process can be discovered in the very beginning and treatment can be started preventing further damage in stages, where the organ's compensatory capacity is still strong enough to recover.

5. Differences to existing methods of sonographic perfusion evaluation

Today RI and PI calculations are the most widely used techniques to quantify flow velocity changes [4-10]. They do not allow conclusions as for the perfusion intensity or volume since the perfused area of the vessel under investigation is not included in the calculation. Even the exact velocities of flow do not need to be measured since the formula refers to two (RI) or three (PI) velocities only which are related to each other to define the velocity change throughout the heart cycle instead of exact velocities. RI = peak systolic velocity - end diastolic velocity / peak systolic velocity and PI = peak systolic velocity - end diastolic velocity / mean velocity of the entire heart cycle.

Contrast enhanced ultrasound (CEUS) can describe the perfusion of larger regions inside organs and thus deliver precise images of typical perfusion patterns of e.g. liver tumours or renal transplant cortical perfusion [11-13]. External influences are relevant concerning the reproducible influx of the contrast enhancer from the injection site to the ROI [14, 15]. The perfusion in CEUS is calculated as the velocity of contrast saturation. The pulsatility of perfusion is not depicted. CEUS thus delivers two parameters to measure: level of saturation and the velocity to reach this level.

The advantages of dynamic tissue perfusion measurement over conventional resistance index measurements and contrast-enhanced sonography (CEUS) are summarized below:

Dynamic tissue perfusion measurement	RI measurement	Contrast enhanced sonography
Measurement of perfusion intensity in all vessels of a larger ROI	Single point measurement in colored vessels	Measurement of contrast enhancement in a larger ROI
Measurement of flow velocities of all pixels in all vessels' transsection	Measurement of flow velocities only in some pixels of a vessel (sample volume)	No flow velocity measurement
Appreciation of heart beat specific flow dynamics	Appreciation of heart beat specific flow dynamics	Loss of heart beat dynamics – saturation curves are calculated
All relevant raw data (i.e. velocities and areas of perfusion) are measured directly during complete heart cycles	Only systolic and enddiastolic velocities are measured	Perfusion intensity is evaluated indirectly from contrast enhancer influx curves (steepness of influx and level of saturation)
Use of unmodified flow data	Use of unmodified flow data	Contrast enhancer as additional source of error
Non-invasive	Non-invasive	Injection necessary
No side effects	No side effects	Rarely side effects
No running costs	No running costs	Additional costs for contrast enhancer (about 92 € per vial)
No age limitation	No age limitation	Not universally licensed for paediatric use

6. Comparison to RI measurements

Resistance index (RI) measurements are widely used to extract a handy quantitative measure from PW (pulsed wave) – Doppler investigations by using to velocity measurements, peak systolic (vs) and enddiastolic velocity (vd) from a single site inside a vessel according to the equation: RI = vs-vd/vs. Despite its broad use the theoretical basis for perfusion quantification remains weak and not surprisingly leads to misleading conclusions. A high RI is commonly linked to a high downstream resistance against flow – often raising the suspicion of a suppressed perfusion while normal RI measurements are referred to as a sign of normal perfusion. Figure 4 clearly demonstrates that this fundamental theoretical misconception also might have obvious practical implications. In the upper line spectral analysis of three peripheral arterial branches of a renal transplant with a stark reduction of peripheral cortical microvessels are shown – averaging to a RI of 0.66. The same value is calculated in the lower line, which stems from another transplant with much better function (serum creatinine 70 vs. 231 µmol/l in the upper line) and abundant vascular signals in the outer cortical periphery. A decision based on RI would attest both transplants a normal "perfusion". DTPM brings out the difference clearly (fig. 5): Perfusion intensity is eight times higher in the proximal cortex in the transplant with a normal function. The insufficient transplant has no peripheral perfusion at all.

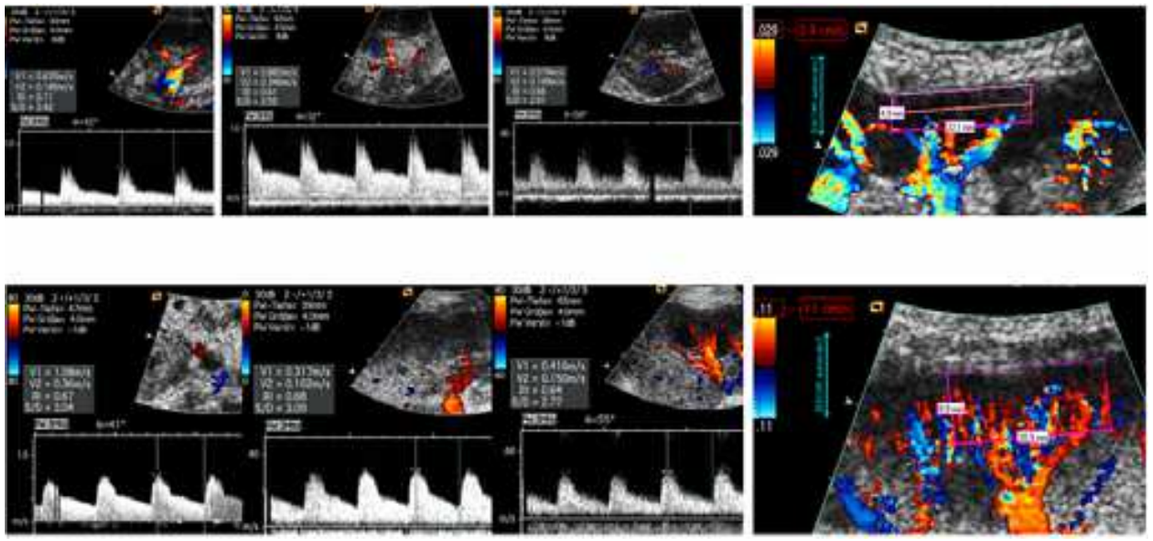

Fig. 4. Two renal transplants compared: upper line insufficient kidney with serum creatinine of 231 µmol/l and normal kidney with a serum creatinine of 70 µmol/l in the lower line. Left: RI measurement in three cortical arteries. Right: Color Doppler sonograms. Insufficient kidney displays a pronounced loss of peripheral perfusion despite more sensible color Doppler setting compared to the kidney below. RI mean values are 0,66 for both transplants

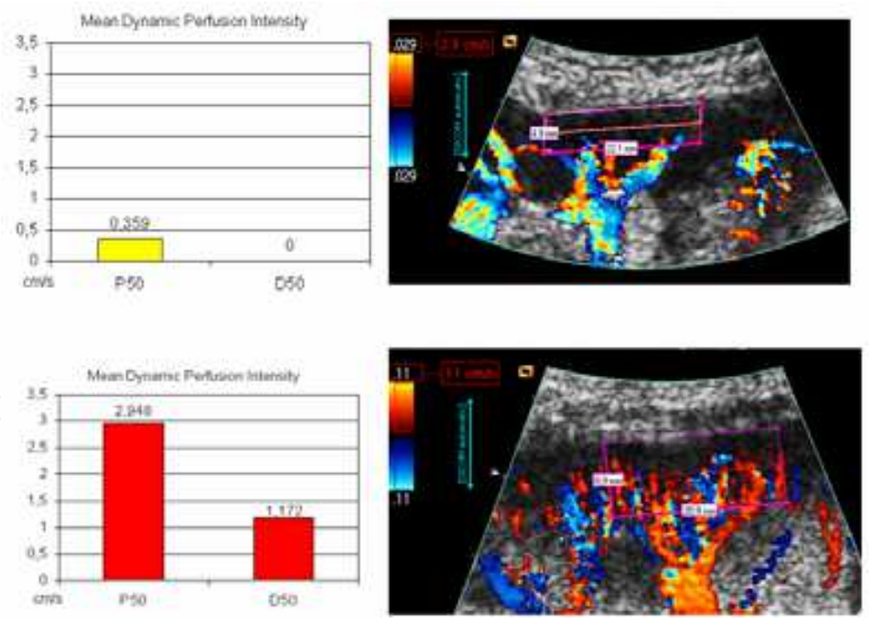

Fig. 5. Same transplants as in fig. 3. DTPM is able to demonstrate a massive difference of tissue perfusion in contrary to RI measurements

Another example for the low power of RI evaluations is figure 6. In a child with acute renal insufficiency due to a hemolytic-uraemic syndrome (HUS), two neighbouring cortical arteries demonstrate vastly different RIs. Depending on which arteries the investigator selects, contradictory conclusions must be drawn from such evaluations. Another seldom-

considered drawback of RI measurements inside tissues is that thin arteries can only be located to interrogate the flow as long as the vessel is still coloured. If perfusion drops significantly, colour signals become weak and disappear at all. These vessels, the most affected, are excluded from evaluation by RI altogether. This must distort the overall evaluation of tissue perfusion if RI measurements are its basis.

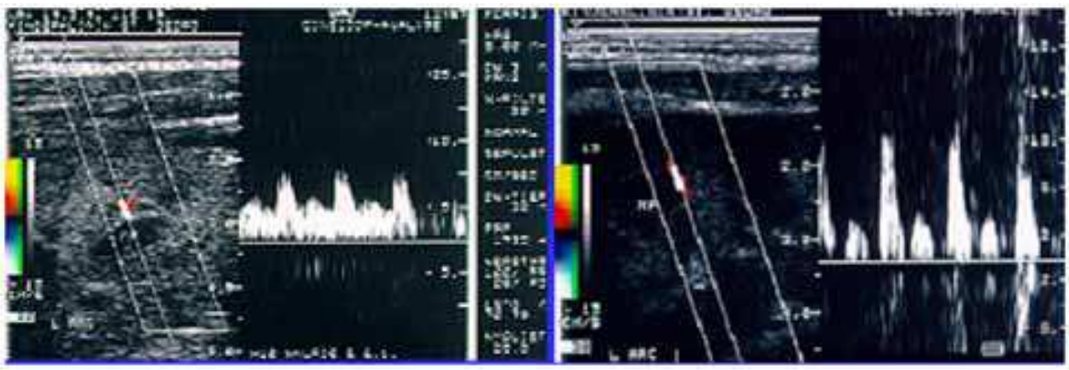

Fig. 6. Misleading RI measurements in a kidney af a child affected by haemolytic-ureamic syndrome. During the same investigation strikingly different RIs are found in intimate neighborhood

The only way out of this dilemma is a method that takes into account simultaneously all flow signals in all vessels inside a larger ROI instead of single vessels, which also takes into account non-perfused areas. These are the fundamentals of DTPM, referring all flow signals inside an entire ROI thus reflecting properly vessel and flow intensity loss in chronic disease. It is just in chronic disease where remaining vessels amidst fibrosed tissue try to compensate the loss of neighbouring vessels by dilatation to feed the "thirsting" periphery and thus exhibit a lower RI than under normal conditions (fig. 5).

7. Phantom flow measurements

A phantom was built to measure the volume flow under externally controlled conditions consisting of a Teflon tube with an internal diameter of 2.0 mm that was placed into a water basin and fixed in a way that the tube was running straight in a steep angle towards the ultrasound transducer that was fixed to a tripod. The tube was perfused with a watery homogeneous rice starch solution.

Colour Doppler videos were recorded under standardized imaging conditions (ultrasound device: S2000, Siemens, Germany, linear transducer, colour Doppler frequency 4 MHz, the angle of the tube towards the ultrasound propagation line was 36°). The pump rate was changed; repeated colour Doppler recordings were made and measured by DTPM.

Two separate investigators independently performed these PixelFlux-measurements from 87 datasets (mean values based on altogether 191 recordings) at 22 different pump rates.

Phantom flow measurements showed an excellent correlation to pump rates (fig. 7) with a Pearson correlation coefficient of pump rate and investigator 1 of 0,987 and 0,991 for investigator 2. Both investigators measurements correlated with 0,997.

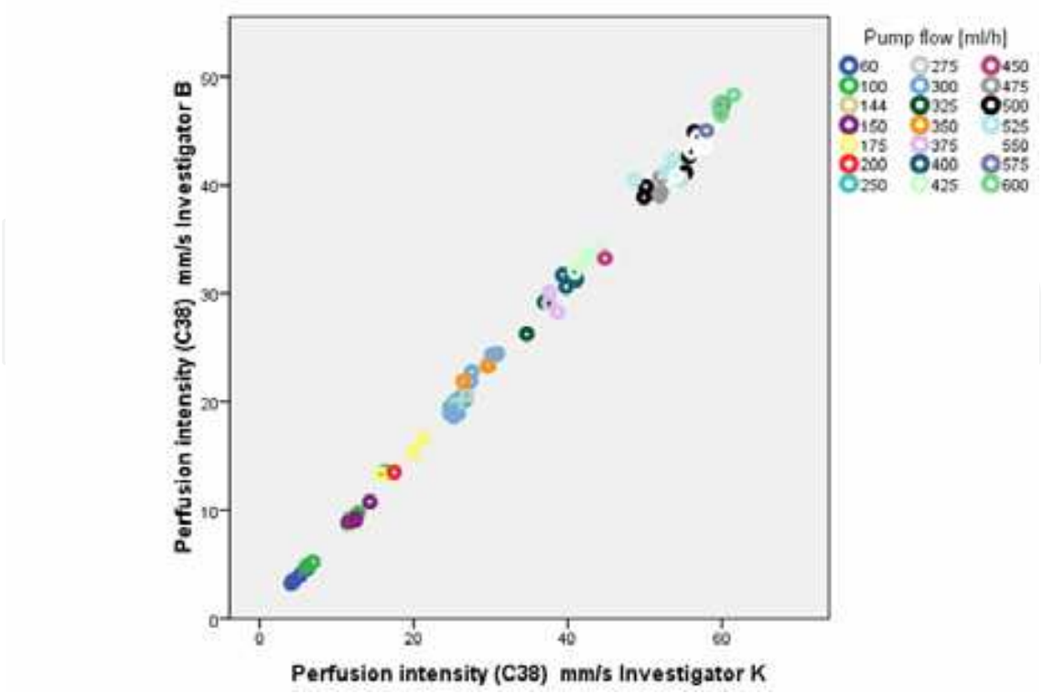

Fig. 7. In a perfusion phantom* DTPM measurements of two investigators were compared. An excellent correlation in-between both investigators and of both investigators to the externally measured flow rate was found. * Homogenized rice starch solution pumped by a precision laboratory pump, Flow volumes measured constantly by a laboratory balance

8. Dynamic tissue perfusion measurement – Applications

8.1 Kidneys

Kidneys are abundantly perfused and are second only to the brain with respect to their blood supply in the systemic circulation [16, 17]. Perfusion measurement is important to detect changes, which precede function loss – the so-called creatinine blind stage of renal insufficiency [18]. For reliable kidney perfusion measurements, it is necessary to adjust the ROI to the typical anatomical pattern of the renal microvessel architecture. The kidney consists of segments, each with an individual blood supply via an interlobar artery. This vessel is crossing the inner parenchyma in-between two neighbouring medullary pyramids to branch off symmetrically into arcuate arteries from which in a brush-like manner interlobular arteries emanate. Such a segment is chosen as the ROI in a way that the feeding interlobar artery runs straight towards the transducer.

The ROI itself is a parallelogram adjusted to the individual kidney's anatomical landmarks, which are as follows: the left upper corner of the parallelogram lies at the renal surface on the watershed line between two segments (i.e. where the interlobular arteries from two neighbouring segments seem to touch each other). The right upper corner then is fixed at the right border of the segment under investigation with the same premises as the first corner. The right lower corner then lies on the right watershed line, which is extended to the surface of the medullary pyramid and ends at the centre of the outer edge of the pyramid. From

there the lower border of the ROI extends to the left pyramid to reach its centre point on its outer border. This is the left lower corner of the parallelogram. This way a symmetric distribution pattern of all branches of this vascular segment is achieved [19]. This parallelogram is divided into horizontal layers (e.g. p50 and d50) encompassing the proximal 50% (p50) or distal 50% (d50) of the ROI's height. Any other layer thickness can be chosen to meet the needs of the investigation (for instance 10 layers with the thickness of 1/10 of the ROI (fig. 13)). These layers thus have a thickness that refers to the overall dimensions of the ROI and are therefore relational layers. In thicker cortices, the layers are thicker than in thinner cortices. Nevertheless, the layers of different kidneys are comparable to each other since they comprise the comparable level of the cortical vascular tree (fig. 8).

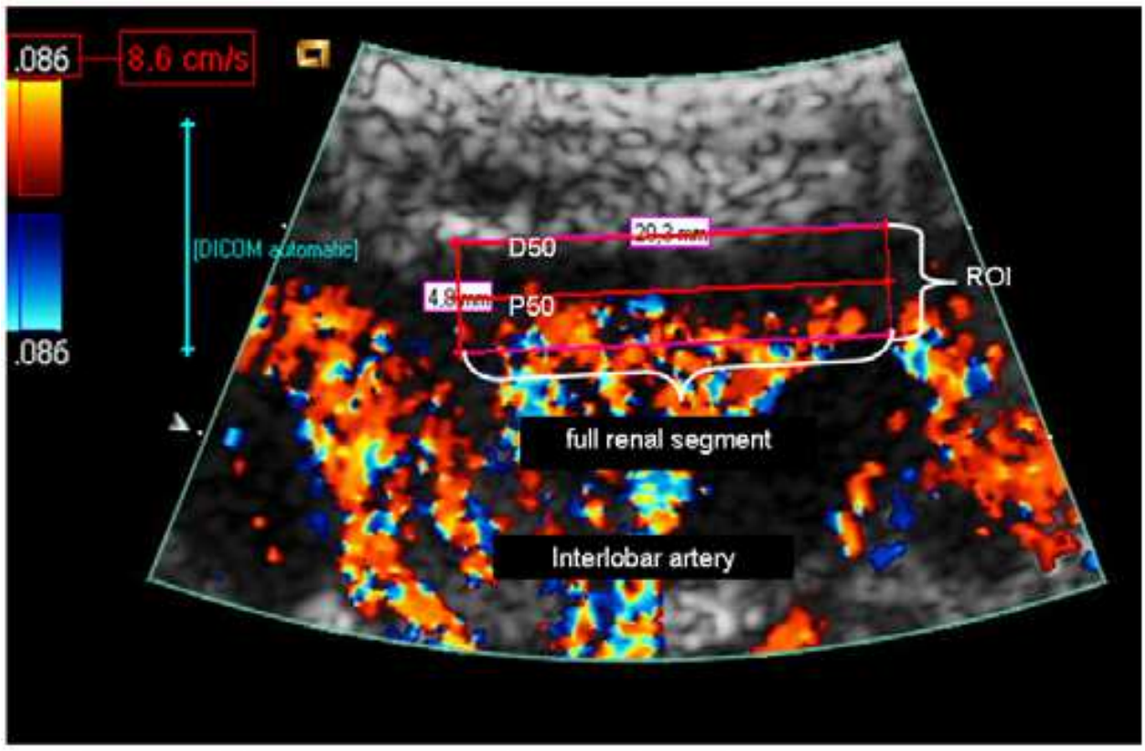

Fig. 8. Example of placing of a ROI in a kidney with indication of the anatomical landmarks to guide the setting

Own investigations yielded a decline of renal cortical perfusion with compromised creatinine clearance (fig. 9). Normal kidneys display a decline of cortical perfusion intensity from central to peripheral cortex (fig. 10) [19]. Inflammation causes a strong hyperperfusion (fig. 11). DTPM can help to differentiate the affection of either right or left kidney – helpful in children and non-communicating patients. Moreover, the different effects of hydronephrotic perfusion loss even in a state of general hyperperfusion due to inflammation can be demonstrated (fig. 11). In kidneys with vesico-ureteral reflux, we found a decline of perfusion inside the peripheral cortical layers, which corresponded to the reflux degree (low grade vs. high-grade reflux) (fig. 12).

In nutcracker phenomenon, a frequent anatomical variant of the course of the left renal vein with sharp narrowing of the vessel between the superior mesenteric artery and the

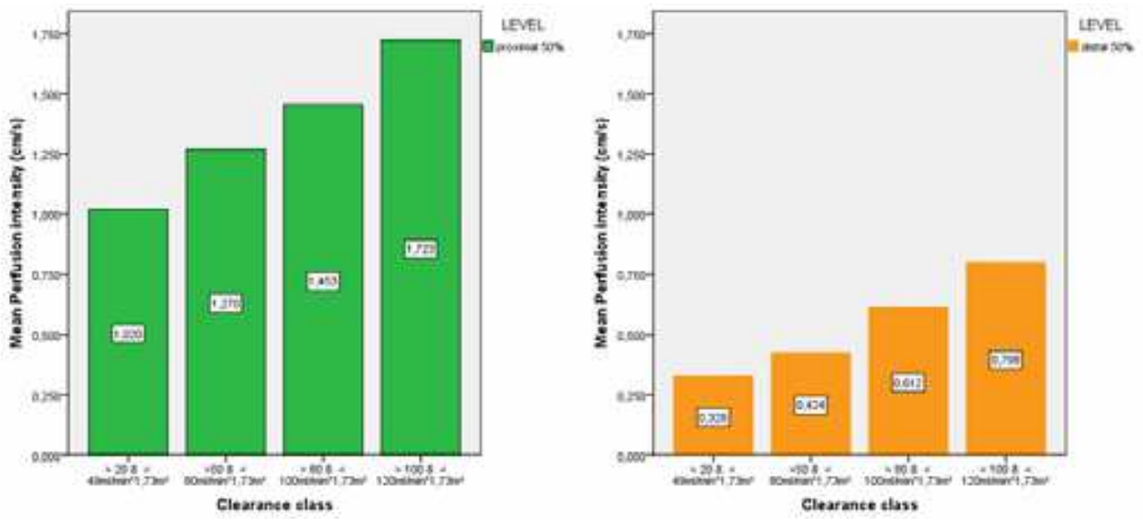

Fig. 9. Constant decline of cortical perfusion with progression of renal insufficiency. Left: proximal cortex. Right: distal cortex

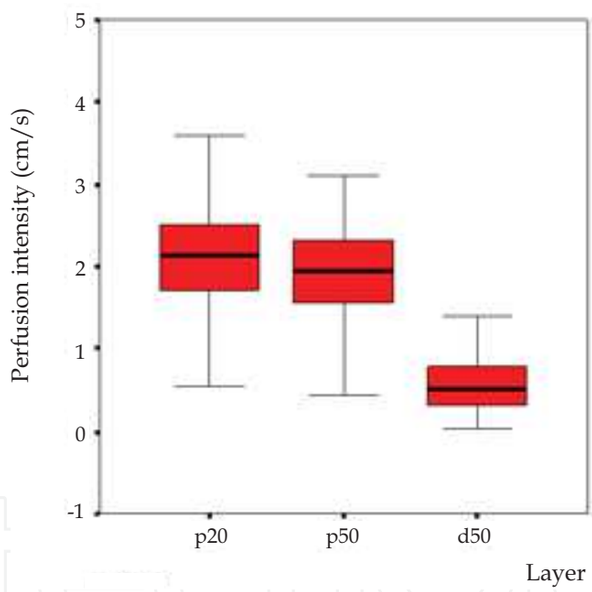

Fig. 10. Decline of renal cortical perfusion from the inner to the outer cortex

abdominal aorta, a venous congestion of the left kidney ensues. Its consequences are often misinterpreted from conventional imaging alone but are nonetheless often disabling for the affected ones. Many patients suffer from chronic and exacerbating abdominal fits of cramping pain. The congested kidney is often swollen and less perfused than the right one. This can be easily demonstrated by DTPM (fig. 13). Perfusion diminution is a signal of insufficient collateral pathways to drain the renal blood from the left side. A treatment with aspirin can either alleviate or often abolish pain and functional disturbances of the congested organs, which have to deal with the massive venous overflow from the left renal vein. Simultaneously with the clinical improvement, a significant increase of left kidney's perfusion can also be measures by DTPM (fig. 14) [20].

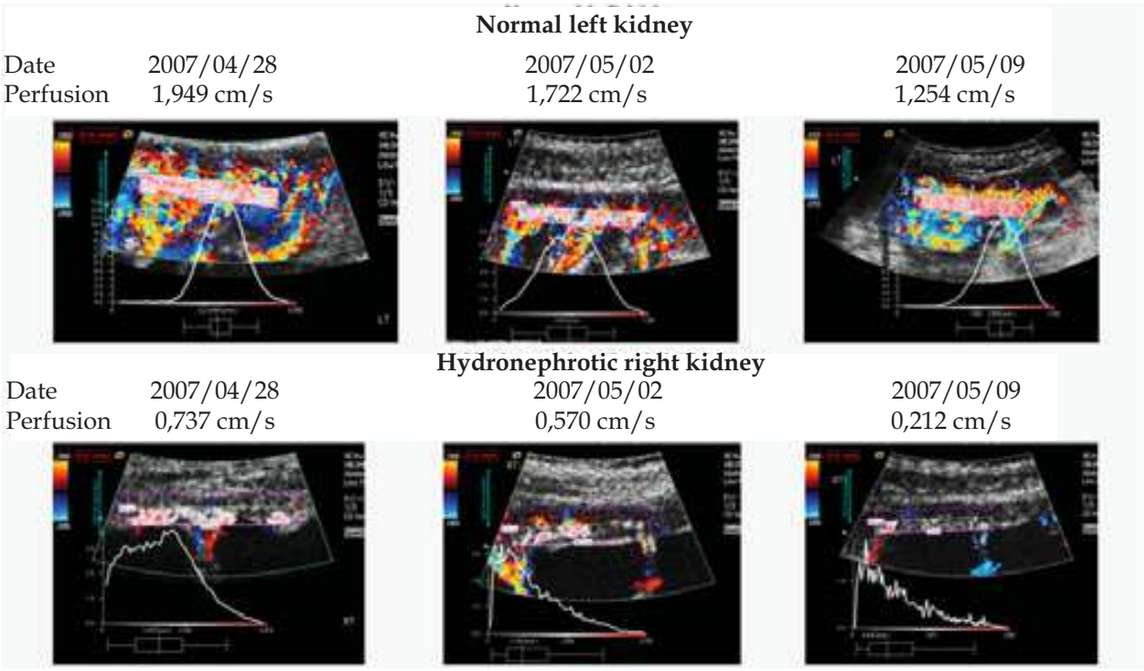

Fig. 11. Differing response of both kidneys towards an bacterial infection in a patient with a right sided hydronephrosis Perfusion intensity in the proximal cortex. MAG3 scintigraphy right kidney: 30% of both kidneys' function. Renal perfusion in a child with a normal kidney on the left and a hydronephritc kidney on the other side. Inflammation due to bacterial infection causes an initial perfusion increase (2007/04/28). With recovery perfusion drops in both kidneys (from 2007/05/02 to 2007/05/09). The decline is more pronounced in the hydronephrotic kidney. Perfusion intensity distribution curves differ markedly between both kidneys pointing to the damage of the microvasculature in the hydronephrotic kidney and a compensatory hyperperfusion trough dilated microvasculature on the left side

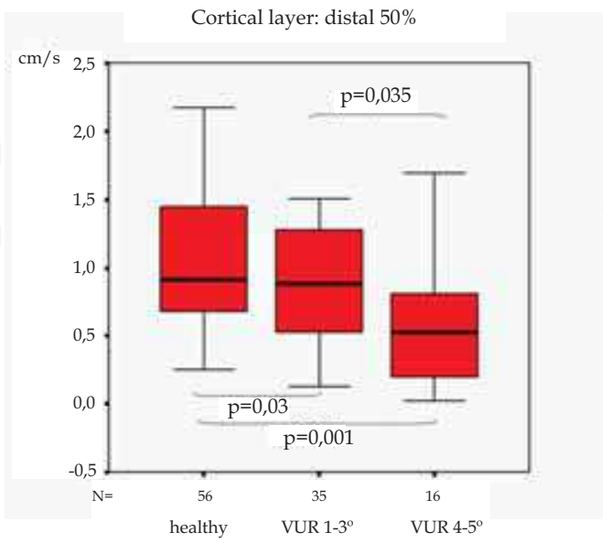

Fig. 12. Diminished perfusion of kidney in vesico-ureteral reflux compared to healthy ones. Compromise of perfusion dependent on degree of reflux

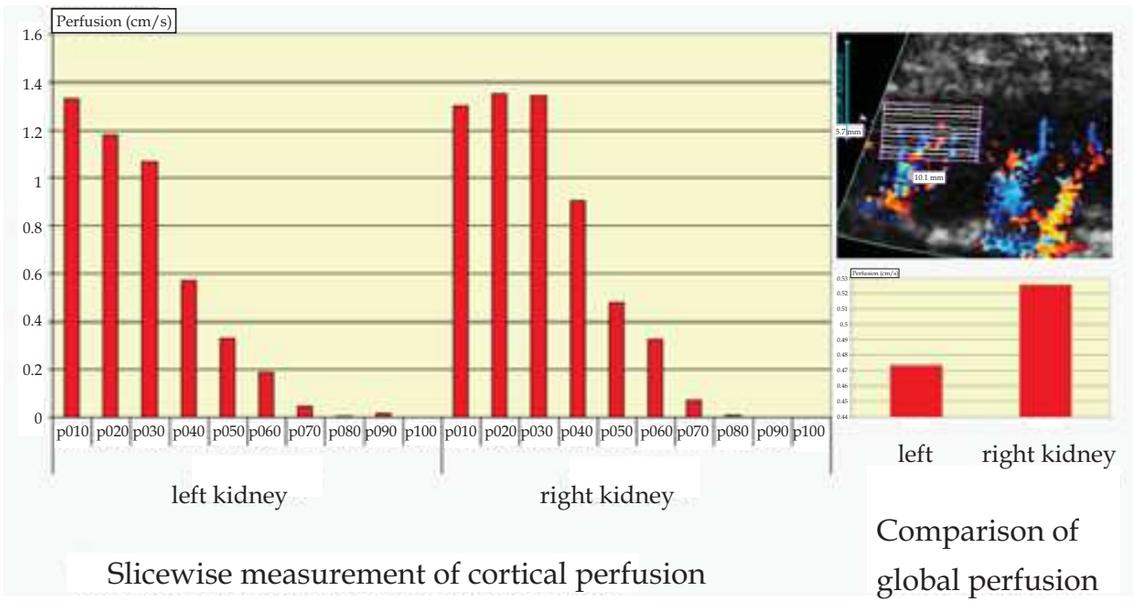

Fig. 13. The nutcracker phenomenon of the left kidney often causes depression of left renal perfusion. Left: Sub-millimeter layers show very precisely the potential of DTPM to describe microvascular perfusion in an unprecedented subtlety. Right: Heavily depressed perfusion of the left kidney in nutcracker phenomenon

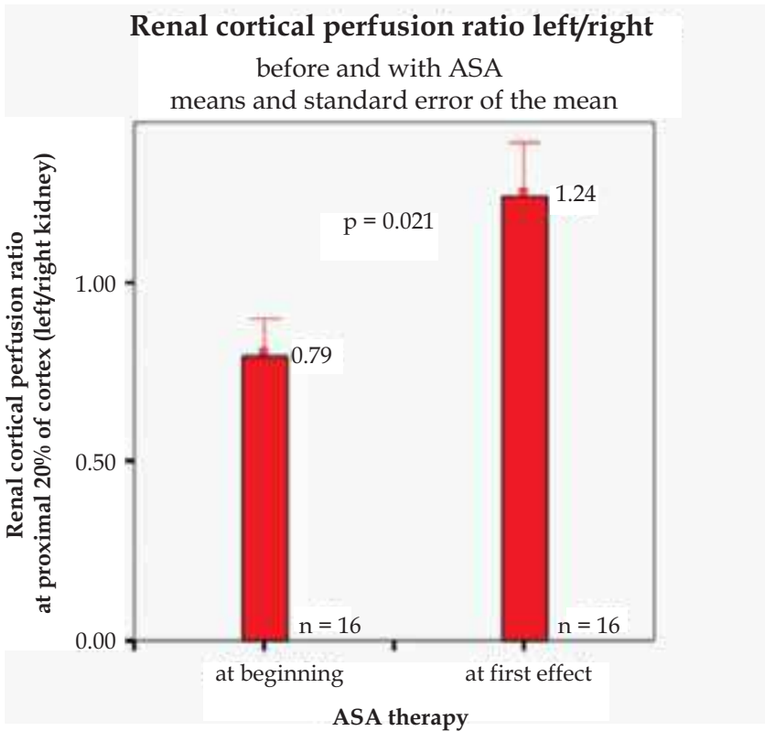

Fig. 14. Effect of aspirin (acetylsalicylic acid: ASA) onto the perfusion of the left kidney. The ratio of left to right kidney perfusion is displayed. After aspirin treatment a significant increase of this ratio can be stated. From [21]

In a preliminary study, we compared kidneys from children with juvenile diabetes of varying duration of disease to kidneys from healthy children with respect to the perfusion drop from central to peripheral cortical layers. Even in an early stage of disease, (no child had microalbuminuria) a highly significant peripheral perfusion loss could be demonstrated in diabetic kidneys (fig. 15).

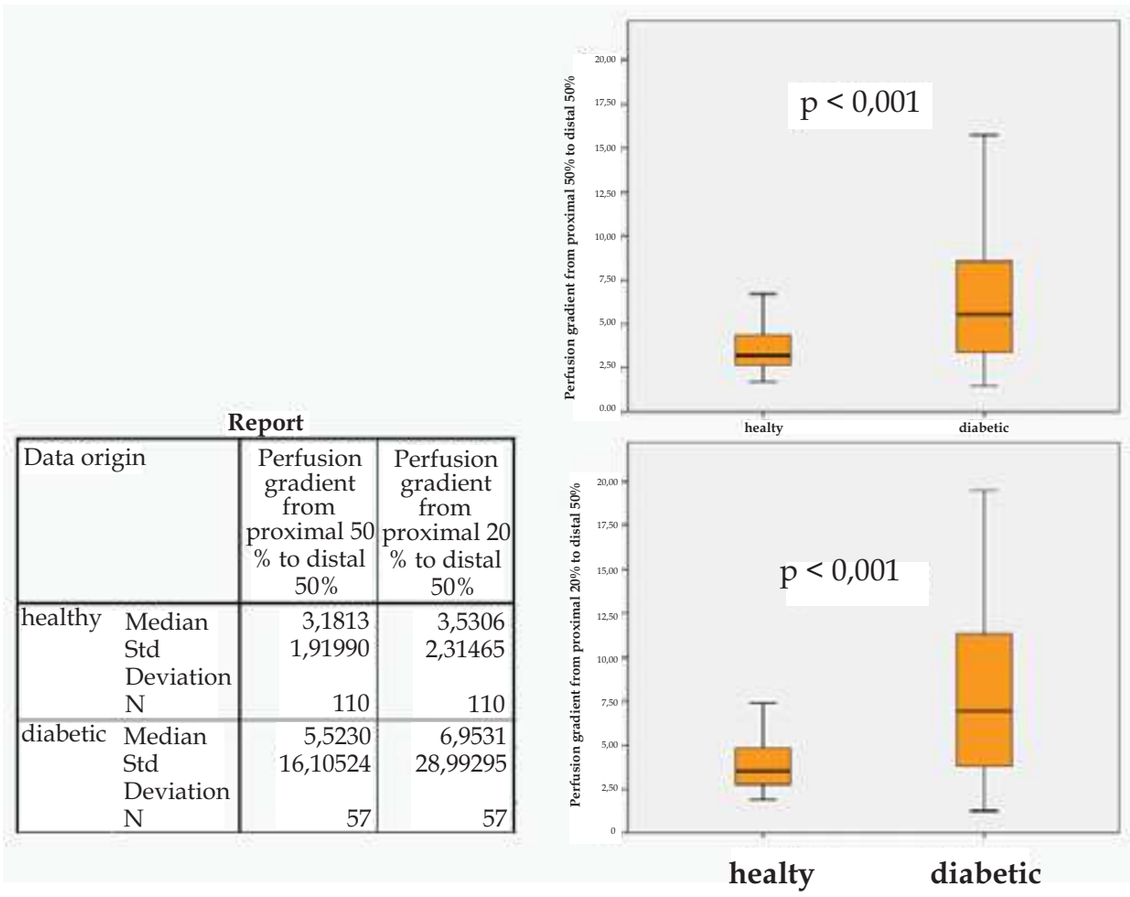

Report

Data origin		Perfusion gradient from proximal 50 % to distal 50%	Perfusion gradient from proximal 20 % to distal 50%
healthy	Median	3,1813	3,5306
	Std Deviation	1,91990	2,31465
	N	110	110
diabetic	Median	5,5230	6,9531
	Std Deviation	16,10524	28,99295
	N	57	57

Fig. 15. DTPM discloses a significant reduction of peripheral to central cortical perfusion in diabetic children compared to healthy ones. The effect is more pronounced when comparing the proximal 20%/distal 50%-ratio (lower diagram) then in proximal 50%/distal 50%-ratio (upper diagram)

9. Renal transplants

Renal transplants are subject to chronic immunological attacks as well as toxic effects of immunosuppressive treatment. Repeated biopsies are today the only way to clarify the creeping changes within the renal parenchyma. We conducted a study on 75 renal transplant recipients, which had a DTPM immediately before their biopsy. Banff criteria were correlated to DTPM results. Some of the very important histological features correlated significantly with perfusion changes [21], pointing to the potential of DTPM for renal transplant long term follow up. RI values were much less instructive (insignificant differences) than DTPM measurements (significant differences) to discriminate varying

stages of peritubular inflammation. Varying grades of transplant Polyomavirus infection were marked with significant increases of cortical tissue perfusion [21]. In another study, we found in children a marked decline of cortical perfusion in allograft cortices beginning already one year after transplantation [22] while the pulsatility of cortical perfusion rose significantly [23]. Recently, it was shown, that intrinsic donor-derived factors are associated with GFR and cortical parenchymal perfusion intensity, measured by DTPM, but not the RI of segmental arteries in renal allografts [24].

10. Bowel

A main area of interest for DTPM is chronic inflammatory bowel diseases. In Crohn disease as well as in ulcerative colitis inflammatory hyperperfusion of the bowel wall could be demonstrated.

Patients with Crohn disease irrespective of disease activity had higher blood flow intensity compared to healthy probands. Mean small bowel wall perfusion intensity was 0.025 cm/s in healthy probands whereas in patients with Crohn disease 0.095 cm/s was found [25]. Large bowel wall perfusion intensity in healthy probands was distinctively less than in patients with Crohn disease (0.012 cm/s vs. 0.082 cm/s, $p < 0.001$) [25]. Conventional evaluation of disease activity by means of activity indices did not clearly distinguish patients with high from those with less pronounced inflammatory hyperperfusion. The correlation of bowel wall perfusion and PCDAI-values was weak albeit significant ($r = 0.349$, $p = 0.001$) [25]. The individual effect of TNF-alpha antibody treatment can be closely followed and treatment regimes can be tailored according to DTPM. Inflammatory activity in fistulas can be measured even after closure of the cutaneous orifice. DTPM can also be used to locate the focus of an abdominal inflammatory process by comparing the perfusion of different structures, which may be involved, but in different extent and activity. So lymph nodes, vermiform appendix, cecum and terminal ileum can be evaluated separately and clear decisions on the main source of complaints can be made. Unnecessary appendectomies can be avoided based on an imaging and perfusion measurements guided approach.

In ulcerative colitis, 14 histological criteria (changes of crypt architecture, depletion of goblet cells, Paneth cells distal of the left colon flexure, lymphocyte infiltration, plasma cells, eosinophils, unspecific inflammatory infiltrates, granulocytes in the lamina propria and lamina epithelialis, crypt abscesses, oedema, erosions or ulcerations, regenerative epithelium , fibrosis, increased cryptal distance to muscularis mucosae) of disease activity were compared to the local perfusion state of the bowel wall. Scores of neutrophil as well as lymphocytic invasion of the wall, crypt abscesses and wall oedema were significantly correlated (in oedema inversely) to the local wall perfusion (fig. 16) [26]. DTPM can add more differentiated and important numerical data, which make imaging data comparable and thus a tool for decision making in a clinical setting. Figure 17 compares histological images, colonoscopic photographs, colour Doppler sonographic images and the results of DTPM at the site where the images stem from. A convincing differentiation of these three bowel segments can be demonstrated by the different perfusion intensities.

Faingold et al. found a trend to decreased intestinal wall perfusion (0.040±0.015 cm/s vs. 0.052±0.029 cm/s) in neonates that died due to hypoxic ischemic injury [27].

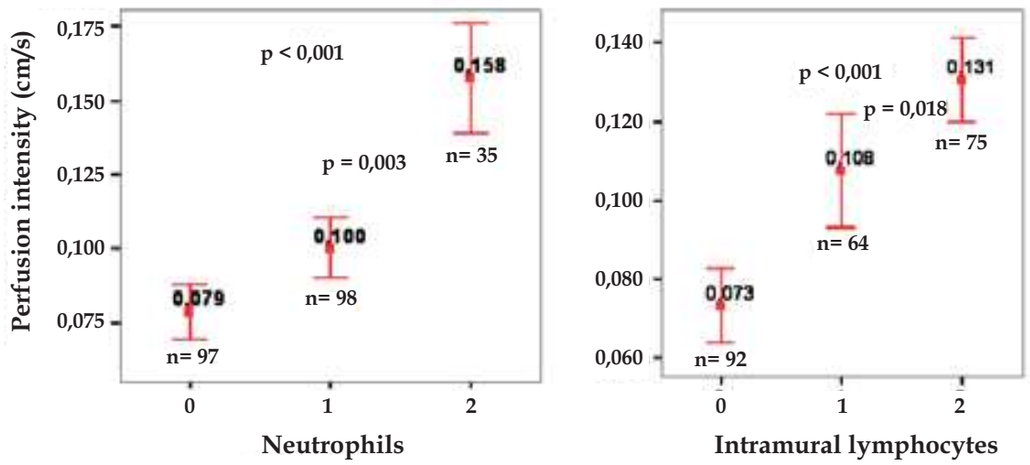

Fig. 16. Large bowel wall perfusion in ulcerative colitis. In ulcerative colitis an increasing score of granulocytic (left) and lymphocytic (right) wall infiltration is reflected by significant increase in wall perfusion

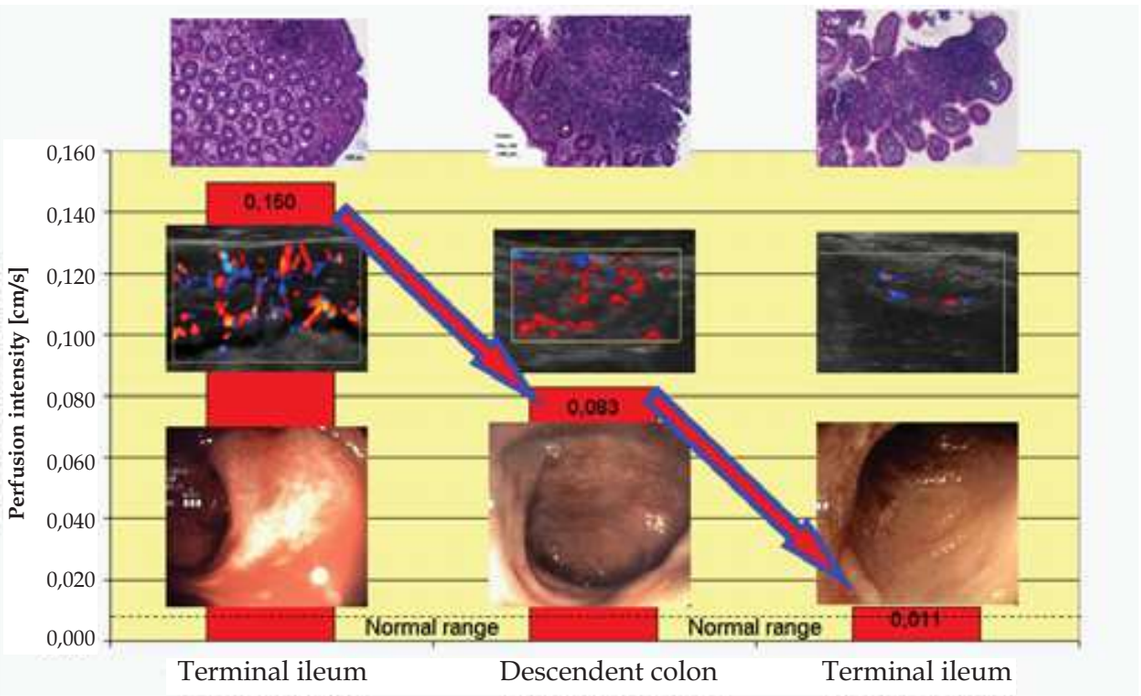

Fig. 17. Synopsis of DTPM measurements (red columns) histological images, color Doppler sonograms and colonoscopic images from three IBD patients and different sites. DTPM differentiates better than all other methods between acutely inflamed and resting bowel segments in IBD patients

11. Lymph nodes

Lymph node perfusion measurement helps to tell inflammatory changes and can provide insight into the dynamics of progression or retreat of the underlying process. Normal lymph

nodes in the neck have a minute but always detectable perfusion, which can be measured accurately. In upper airway infections, lymph nodes do not react with a hyperperfusion whereas lymphotropic EBV infection resulted in a marked increase of perfusion (fig. 18) [28].

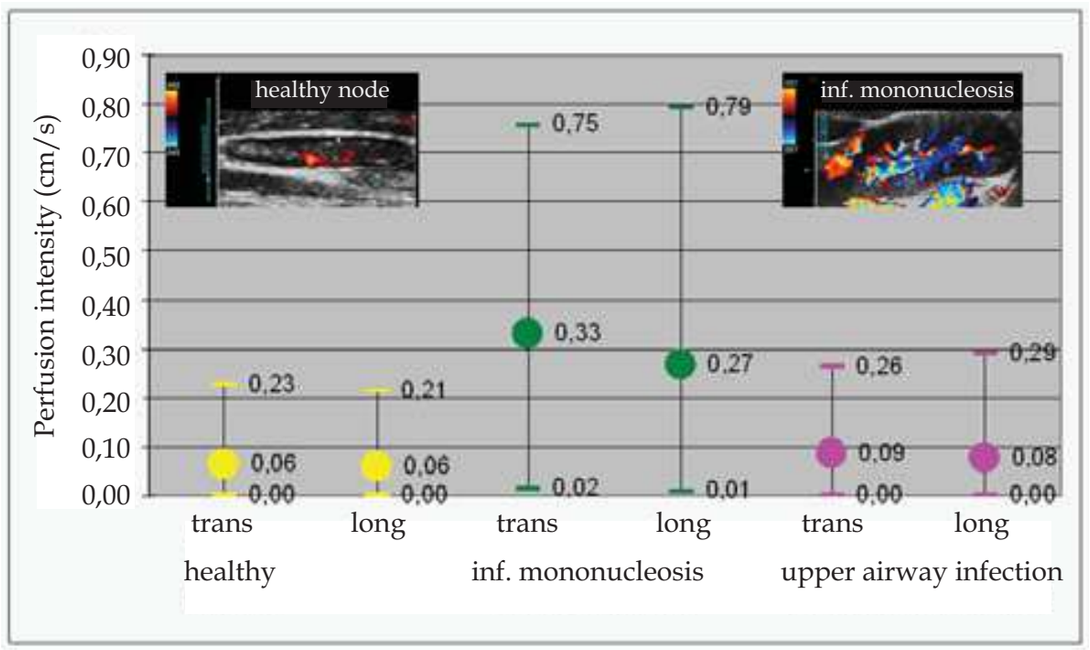

Fig. 18. Lymph node perfusion as seen in DTPM: no differences exist between longitudinal (long) and transverse (trans) sections of the nodes. Infectious mononucleosis raises cervical node perfusion significantly (green symbols) compared to nodes from healthy probands (yellow) in contrast to nodes in acute upper airway infections (pink). Insets: left: normal node in color Doppler Right: Node in infectious mononucleosis (EBV-infection)

12. Muscle

A muscle perfusion measurement is feasible with the demonstration of a marked increase during exercise and steep decline afterwards in athletes (fig. 19). The perfusion was measured in the M. rectus femoris in a horizontal section before during and after exercise along with the measurement of serum lactate and a self-estimation of subjective workload (fig. 20).

In aged patients, an increase of muscle perfusion of the M. biceps brachii was demonstrated during an exercise program to foster rehabilitation.

13. Thyroid

Reproducibility of thyroid DTPM between two investigators is significant (fig. 21).

Thyroid perfusion is strongly increased in thyreoiditis (fig. 22). It is not yet clear however, if the amount of perfusion is paralleled by conventional laboratory parameters or clinical symptoms.

Thyroid nodules differed with respect to their distribution of perfusion according to their biological behaviour. Comparison of perfusion intensities obtained from peripheral and central parts of the nodules revealed that, in non-neoplastic nodules the peripheral flow was more intense than the central flow and, on the contrary central flow was more prominent than the peripheral flow in neoplastic nodules ($p<0.005$) [29].

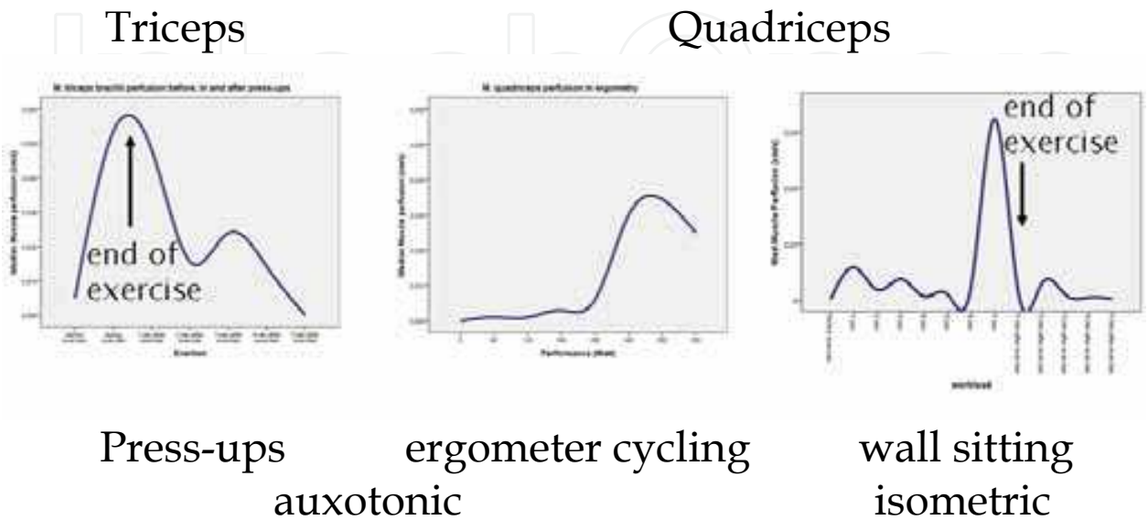

Fig. 19. Significant muscle perfusion increase in 13 athletes – maximal exercise. DTPM reflects the perfusion in muscles before, during and after physical exercise in various settings. Auxotonic as well as isometric exercises cause a strong perfusion increase. After exercise perfusion drops sharply

		Duration of exercise	Heart rate
Muscle Perfusion	Spearman corr. Coeff.	**,535**	**,469**
	Sig. (2-tailed)	**,000**	**,000**
	N	61	61

Fig. 20. Correlation of quadriceps perfusion during ergometer cycling. Exercise induced muscle perfusion correlates significantly to duration of exercise and heart rate

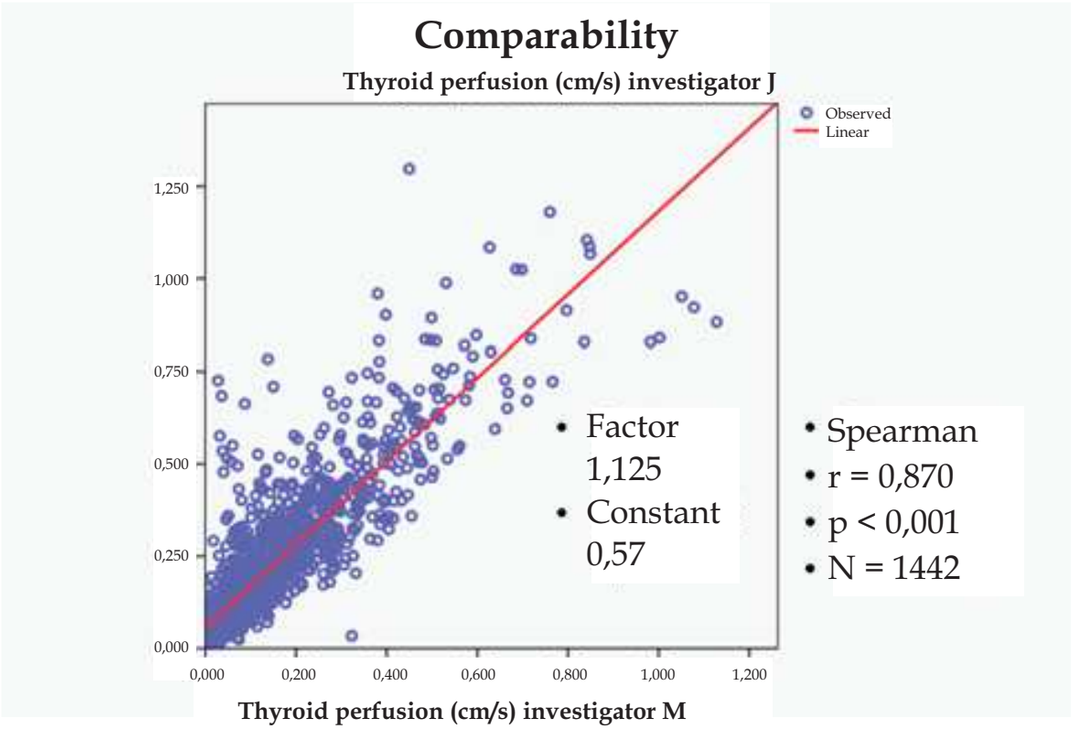

Fig. 21. Thyroid perfusion in 1142 measurements – low interobserver variation and highly significant correlation between both investigators

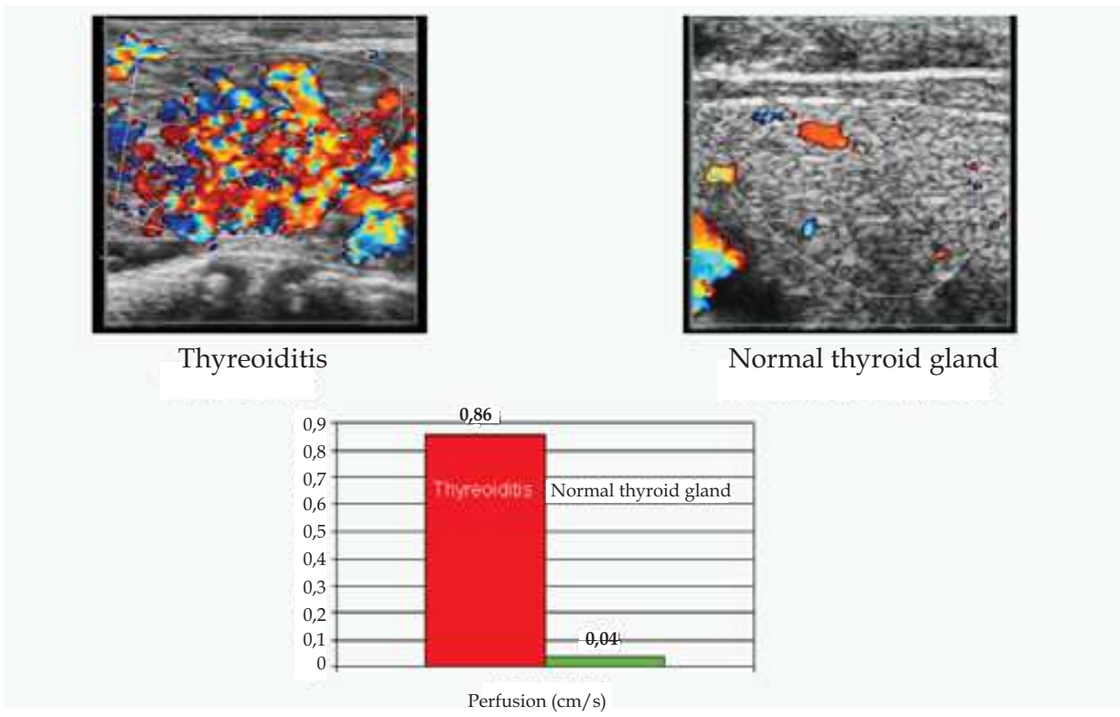

Fig. 22. Example of ample perfusion increase in thyroiditis – color Doppler sonograms and corresponding DTPM values are displayed

14. Tumours

Tumour perfusion evaluation by DTPM is also feasible and defined regions such as tumour core and periphery, whose size can be predefined, e.g. as concentric regions. This can uncover central tumour necrosis or ischemia, which might be relevant for treatment decisions. Hypoxia due to ischemia is a factor of chemo- and radioresistance of tumours [30-32]. Therefore, it might be useful to monitor tumour perfusion in separated shells.

In a series of metastatic tumours of the neck, a direct correlation of tumour perfusion measured by means of DTPM and directly measured tumour oxygenation could be demonstrated (fig. 23) [33]. In hypoxic tumours perfusion was significantly lower compared to normally oxygenated ones (fig. 24). Moreover, the pulsatility of tumour perfusion differed significantly between groups with different stages of metastasis (fig. 25) [33]. These results may be interpreted as a change of tumour stroma. The more densely packed the stroma is the higher the pulsatility is, since the distension of small vessels is influenced by the pressure change during a heart cycle on the one hand but on the other hand by the resistance against the widening of a vessel by the surrounding structures and their stiffness.

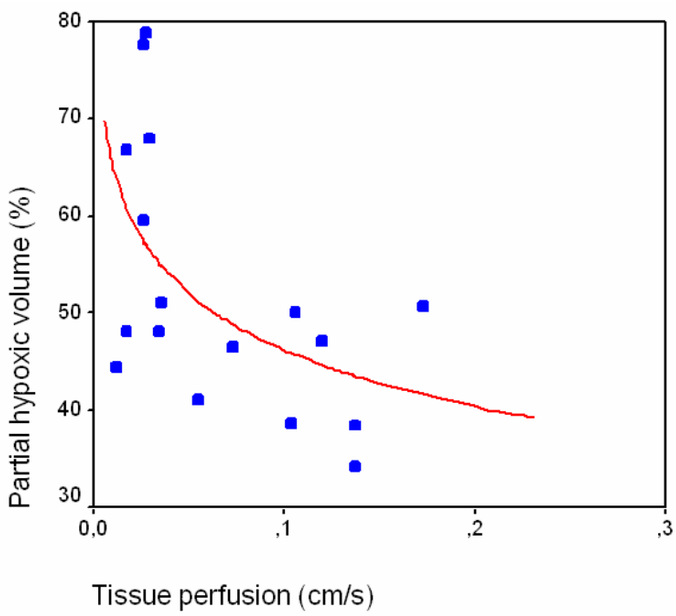

Fig. 23. Significant correlation between directly measured hypoxic volumes in metastatic lymph node tumors of the neck (Eppendorf histiograph) and DTPM (from [2])

15. Foetus

The foetal perfusion has to meet the needs of the rapidly growing organism, to deliver oxygen and nutrients in order to permit a normal intrauterine growth. Among other causes placental insufficiency is an important reason for disturbed intrauterine growth, resulting in intrauterine growth retardation (IUGR) and postnatal complications. The evaluation of foetal perfusion today is based in daily practice on the calculation of RI and PI in large arteries, mainly the umbilical, the cerebral arteries and the aorta, sometimes supplemented by flow pattern evaluations in the venous duct [34, 35]. In the eighties of the last century, first

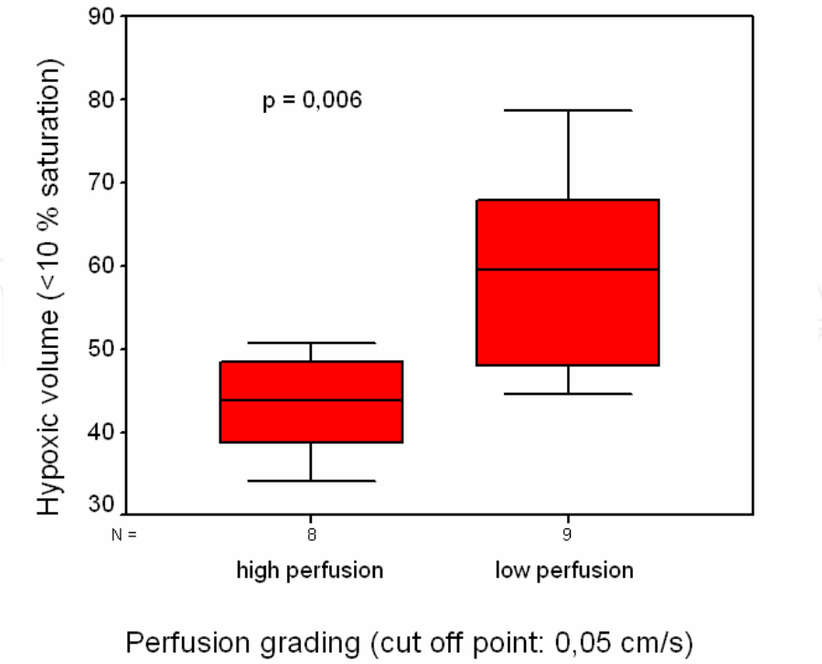

Fig. 24. Oxygenation differences in relation to tumor perfusion. Less perfused metastatic lymph nodes in the neck (cut off in DTPM: 0,05 cm/s) have a significantly higher hypoxic volume than well perfused nodes (from [2])

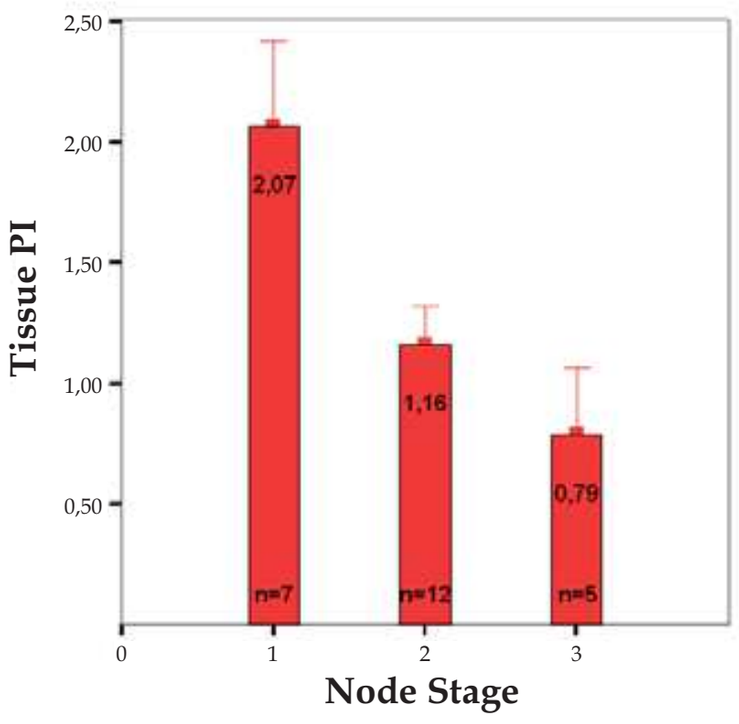

Fig. 25. The Tissue Perfusion Pulsatility Index (TPI) falls significantly with increasing N-stages of the nodes (from [2])

attempts tried to quantify the umbilical venous flow volume with the aim to evaluate the foetal perfusion in quantitative terms [36, 37]. These studies were not continued because of limited reproducibility [38]. Nevertheless, these studies targeted at a parameter – volume flow –, which has a much better rationale than the popular and easy to measure RI and PI. The early studies were flawed mainly by two limitations, which could not be overcome with two-dimensional sonographic techniques. First the angle correction of flow velocity in space and second the non-circular shape of the transsection of the umbilical vein (UV).

Spatial angle correction is but pivotal in this setting, because the UV is continuously winding around the umbilical arteries and the whole cord is irregularly bent within the amniotic cavity. Two-dimensional images thus may allow an angle correction within the frontal plane but this can be vastly misleading. Depending on the sagittal angle the true and only relevant spatial angle can differ substantially thus leading to unpredictable errors of the volume flow calculation, when unknown. The second source of error was the universal assumption, that the UV is a round tube. The investigators tried to depict a straight running venous segment with parallel borders to apply the formula for circular area calculation in order to multiply this area with the mean flow velocity which was traced with a pulsed-wave- Doppler instrument in the centre of the vein.

These sources of error combined in an unpredictable manner and caused the refusal of this approach.

The technique of DTPM combined with the modern three-dimensional imaging techniques can resolve all of these imponderabilities. We developed the three-dimensional, spatial angle corrected umbilical vein flow volume measurement, which is outlined below.

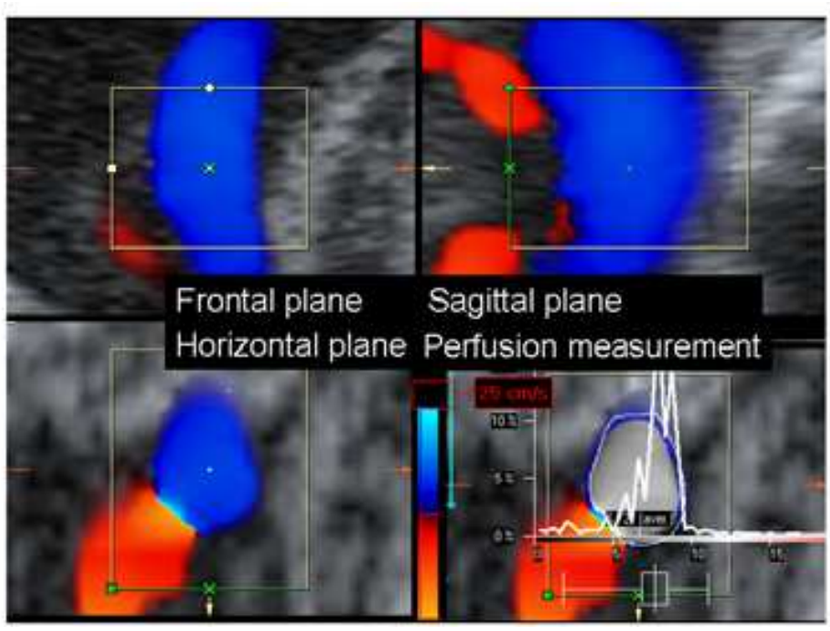

Fig. 26. Example of a spatially angle corrected fetal volume flow measurement in the umbilical vein. A 3D-dataset is shown displaying three perpendicular imaging planes. The horizontal plane is used for DTPM (right lower quarter): False color map of the venous flow. From these data the flow volume is directly calculated by the PixelFlux-software

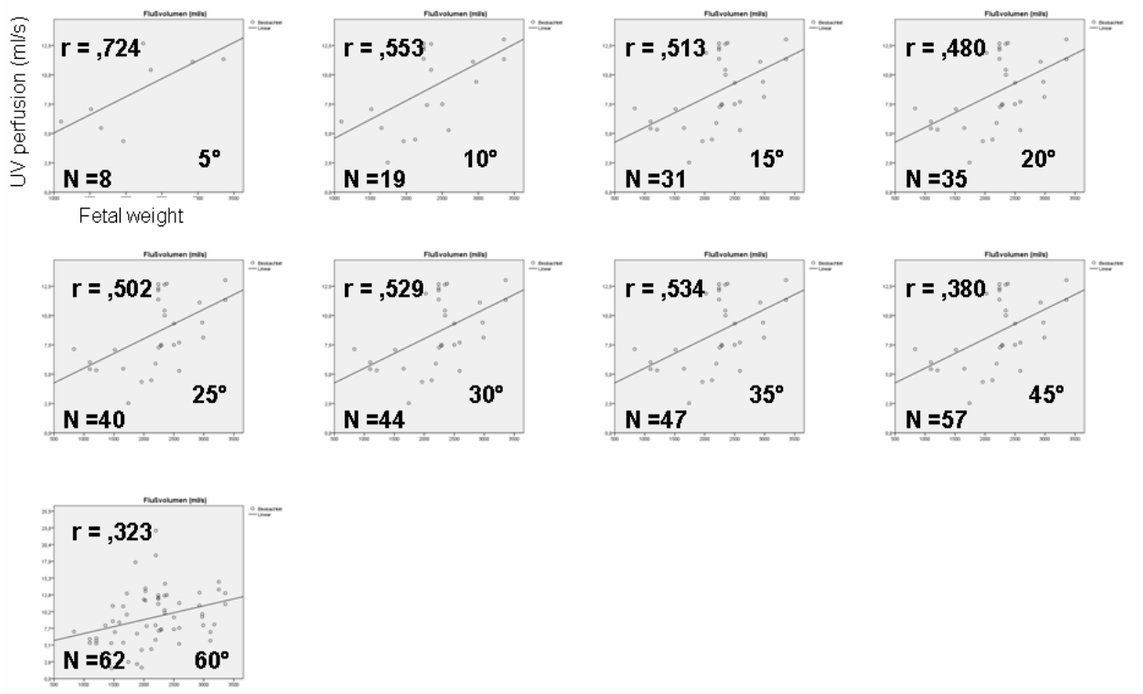

Fig. 27. DTPM reveals a significant correlation of fetal volume flow and fetal weight. This correlation improves significantly with reduction of the spatial angle (specified within each diagram)

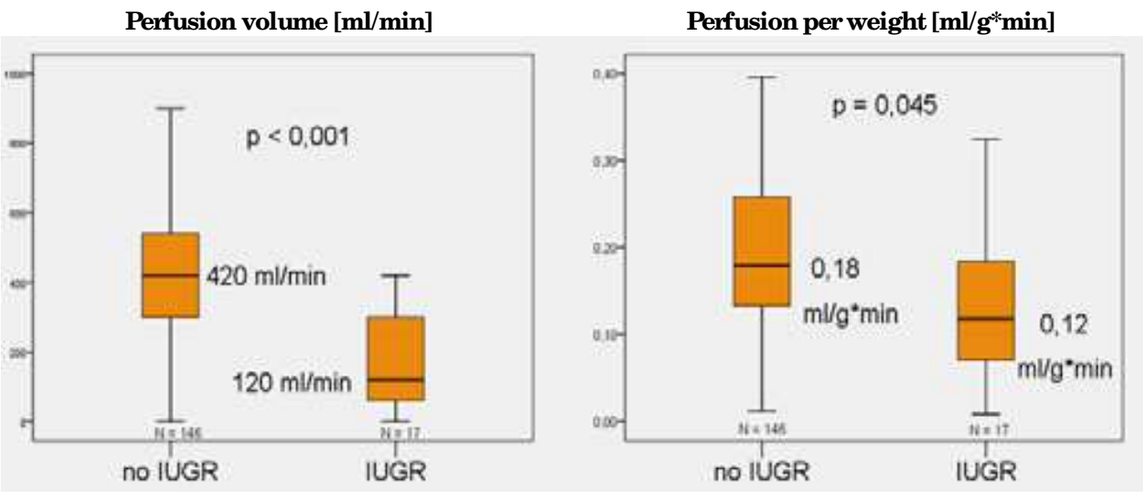

Fig. 28. A significant reduction of fetal perfusion per gram fetal weight could be demonstrated by DTPM in fetuses with intrauterine growth retardation (IUGR) compared to normal children

To achieve best results the umbilical cord should be recorded in a 3D-colour Doppler sweep so that the vein is running in a steep angle towards the transducer. The data block is then scanned with a 3D-manipulation software (4Dview, GE) by parallel shifts of the frontal and sagittal images to search for a transsection of the UV in the horizontal plane, which is clearly cut, has distinct borders and is not taken from a segment of the vein with strong bending (fig.

26). In this plane both velocity as displayed by a certain colour hue and shape of the vessel's cross section are distorted by a stretching factor which is equal to the cosine of the spatial angle between vessel's course and the ultrasound waves' propagation line – the so called Doppler angle α. While the area is stretched by the reciprocal of cos α the velocity is virtually reduced by the by multiplication with cos α (proof see chapter 18. Addendum on page 27). Therefore, direct calculation of true flow volumes directly from measurements within the horizontal plane is possible. This is accomplished by the DTPM software PixelFlux. The reproducibility of these measurements in a clinical situation lies in the range of around 6 % and less, if exclusively data with steep spatial Doppler angles are allowed (own unpublished data).

A significant correlation of such volume flow measurements with fetal weight could be demonstrated (fig. 27) [41] that was the better the steeper the spatial angle could be arranged. Moreover, in a preliminary study a significantly diminished flow volume per gram fetal weight could be shown (fig. 28).

16. Miscellaneous

In animal models, numerous reports underscore the interest in DTPM, especially in the field of theriogenology. The functional status of the bovine ovary (evaluated by the plasma progesterone concentration during the oestrous cycle) could be better correlated to luteal blood flow than to luteal size ([39]. The course of luteal perfusion mirrored progesterone levels much more readily than the sheer size of the corpus luteum. The perfusion measurement of the ovary in cows could differentiate between varying courses of progesterone plasma levels [41]. Perfusion measurements of the follicle, the corpus luteum and the uterus yielded differing responses in cows undergoing synchronization of ovulation [42]. They helped to explain the effect of human chorionic gonadotropin onto the progesterone synthesis and luteal blood flow [43], were useful in monitoring luteal perfusion during pregnancy and after embryonic loss [44] and could be used to tackle a variety of interactions between hormone production, luteal blood flow and gene expressions in luteal tissue [45].

In another study on the regulation of follicular development in cows DTPM demonstrated significant correlation with the follicular NO concentration and Estradiol (E2)/Progesterone (P4) ratio in those follicles, which developed to the dominant follicle in the ovary [46].

In milking of cows, a significant increase of utter perfusion was measured after 15 – 30 min to settle down after 45 min to the basic, pre-milking values. These basic values but differed considerably among the animals [47].

DTPM helped to describe the periurethral vascularity in women [3], was used to estimate the effect of periprostatic vascularity on the effect of HIFU in prostate cancer [48], proved to be more sensitive than computer assisted B-mode image analysis in testicular torsion and showed clearly a perfusion decline within two hours after torsion [49].

Perfusion measurements of the basal ganglia using DTPM in neonates with hypoxic ischemic encephalopathy (HIE) treated with therapeutic hypothermia demonstrated significantly higher perfusion values in neonates that died compared to the survivors (0.226± 0.221 cm/s vs. 0.111±0.082 cm/sec; p=0.02) (fig. 29). DTPM values also were higher

in nine neonates with MRI showing moderate to severe injury (0.142±0.070 cm/s vs. 0.072±0.080 cm/s; p=0.04). DTPM opens a window to better understand reperfusion injury in HIE [49].

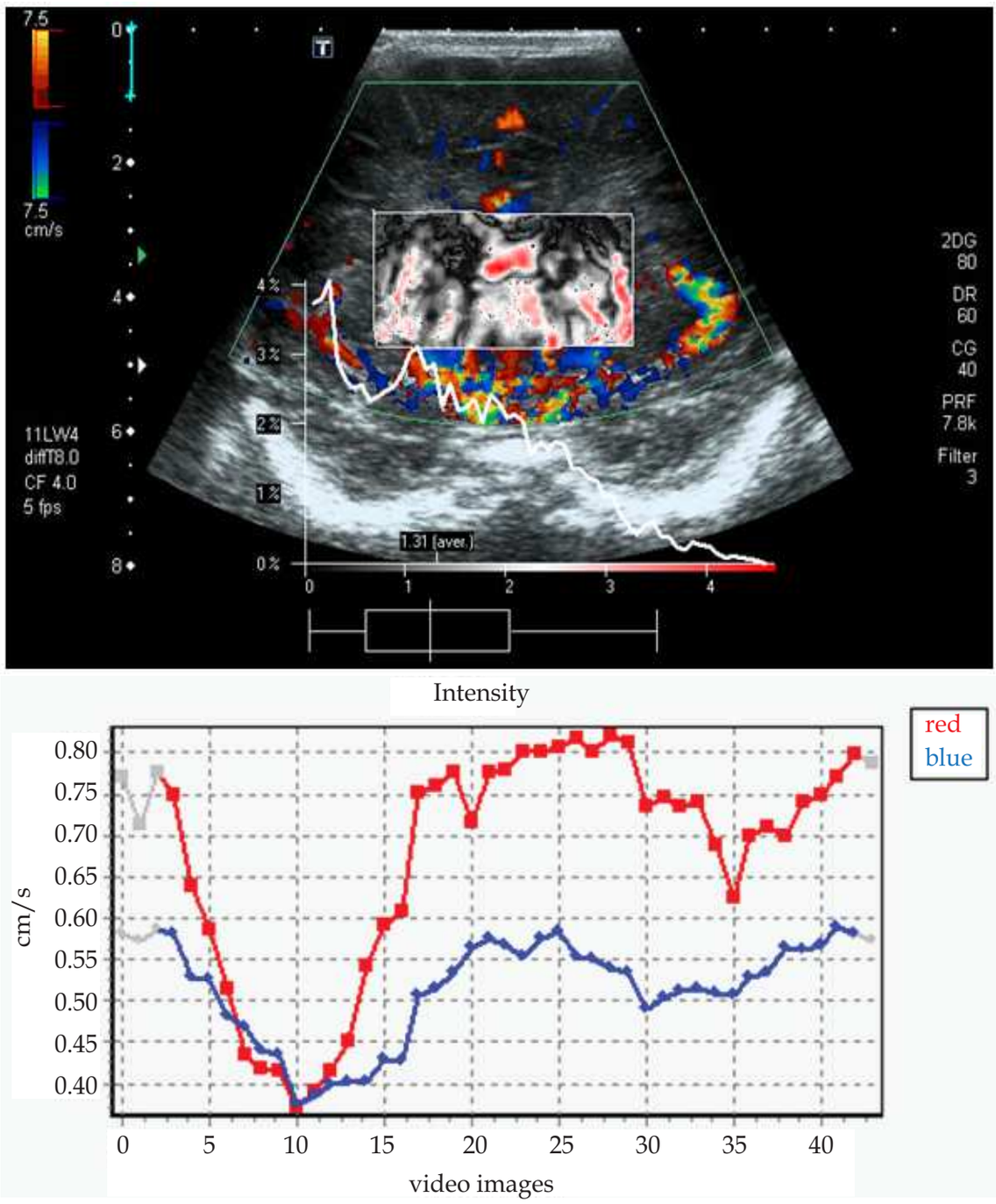

Fig. 29. Example of a DTPM of basal ganglia in a newborn. Upper part: false color map of the basal ganglia and distribution curve. Lower part: Perfusion intensity course during one examination. (Image and measurement courtesy of Dr. Ricardo Faingold, Montreal)

17. Summary

DTPM offers a universally applicable approach to tissue perfusion measurement as far as sonographic depiction of tissues is possible. So far, inaccessible details of perfusion intensity, perfusion distribution, perfusion gradients within a certain vasculature open a widow to an individualized evaluation of the specific pathophysiological situation. Treatment efforts can be evaluated according to their effect on perfusion. Besides these intrinsic advantages, the technique requires no additional hardware, is non-invasive, needs no specific preparation of the patient and thus can be recommended for a broad array of clinical applications.

18. Addendum: Proof of the congruence of the true flow volume and the flow volume calculated from the horizontally projected velocity and area of any vessel

True volume flow calculation becomes feasible with three-dimensional colour Doppler data.

True volume flow calculation means the exact calculation of the blood flow volume running through any vessel which is cut perpendicularly.

Our method of true volume perfusion measurement in vessels cut by the horizontal plane in any spatial angle is described and proven below.

The spatial angle, which is the angle between the vessel and the ultrasound propagation line, influences simultaneously the stretching of the shape of the vessels' cross-sectional area as well as the change of the recorded flow velocity. Figure 30 displays the respective situation schematically. The blood vessel (yellow rectangle) runs with the Doppler angle α towards the ultrasound propagation line (blue line). The horizontal imaging plane, which is calculated during the three-dimensional ultrasound imaging, cuts the vessel. Line a' is the stretched vessel's diameter as it can be seen in the horizontal plane. Vector b is the original flow velocity within the vessel. Due to the Doppler angle α the recorded velocity is displayed with the value for vector b'. This means, the color hue of b' is darker, representing a lower velocity as if vector b would be displayed in its appropriate color. This is the well known Doppler effect $\left(fd = 2 * fo * v_t / c * \cos\alpha\right)$, which reduces the recorded velocity according to the cosine of α.

The real flow volume per time (V) of a circular vessel is calculated as

$$V/t = \pi/4 * a * a * \vec{b} \tag{1}$$

// $\pi/4 * a * a$ calculates the circular area of the perpendicularly cut vessel

The oblique transsection of a round vessel, a vessel running not perpendicularly towards the horizontal plane, results in stretching of the circular vessel's round cross-sectional area in the direction of the projection vector of the spatial angle of this vessel with the horizontal plane. This results in an ellipse which longer axis is represented by a', the stretched projection of a onto the horizontal plane (Fig. 30). The shorter axis is equal to the original diameter of the vessel. It remains unstretched since no angulation occurs.

It is therefore possible to consider the change of diameter a towards a', the long axis of the ellipse in order to describe the change of the horizontally projected cross-sectional area of

the vessel. The change of the circular area towards the elliptical area is thus equal to the stretching factor a'/a.

The other relevant change is the reduction of the displayed flow velocity compared to the original velocity b, the reduction factor is b'/b.

It is now claimed, that the flow volume V′ per time, which is passing through the horizontal plane in direction of the vessel, calculated by multiplying the elliptical area $\left(A = \pi/4 * a * a'\right)$ with the flow velocity b′ of the vessel in the horizontal plane is equal to V per time, the flow volume passing through the perpendicularly cut vessel in the same time.

Claim:

$$V' = V \tag{2}$$

Proof:

$$V'/t = \pi/4 * a * a' * \vec{b}' \tag{3}$$

// $\pi/4 * a * a'$ calculates the elliptic area of the horizontally cut vessel
a: short axis of the ellipse
a' : long axis of the ellipse

The depiction of the horizontally cut vessel shows the velocity $\vec{b}'$ and a stretched vessel diameter a'.

The triangle ABC is rectangular, since the blood vessel is a rectangle, a perpendicularly cut circular straight vessel. Doppler angle α is complemented to 90° by the angles DAB and FAC since the ultrasound propagation line (blue line running through F) runs perpendicular to the transducer's surface and thus the horizontal imaging plane. Both angles are thus equal and named β. Angles FAC and CAB add to 90° since again the ultrasound propagation line runs perpendicular to the horizontal imaging plane. Thus angle CAB is α again, the Doppler angle.

$$a' = a / \cos\alpha \tag{4}$$

$$\vec{b}' = \vec{b} * \cos\alpha \tag{5}$$

by inserting (3) and (4) into (2) results (5)

$$V' = \pi/4 * a * a/\cos\alpha * \vec{b} * \cos\alpha \tag{6}$$

which is (6) after cancelling cos α

$$V' = \pi/4 * a * a * \vec{b} = V \text{ see (1)} \tag{7}$$

thus

$$V' = V \tag{8}$$

q.e.d.

This means, that it is possible to calculate the true flow volume of all vessels cut horizontally from the depicted flow velocities[1] and the pixelwise calculated cross-sectional areas[2] directly, thus compensating any spatial angle. Both measurements ([1] and [2]), are carried out automatically by the PixelFlux-software, which delivers thus true flow volumes of all vessels in any tissue section cut horizontally in three-dimensional color Doppler ultrasound data.

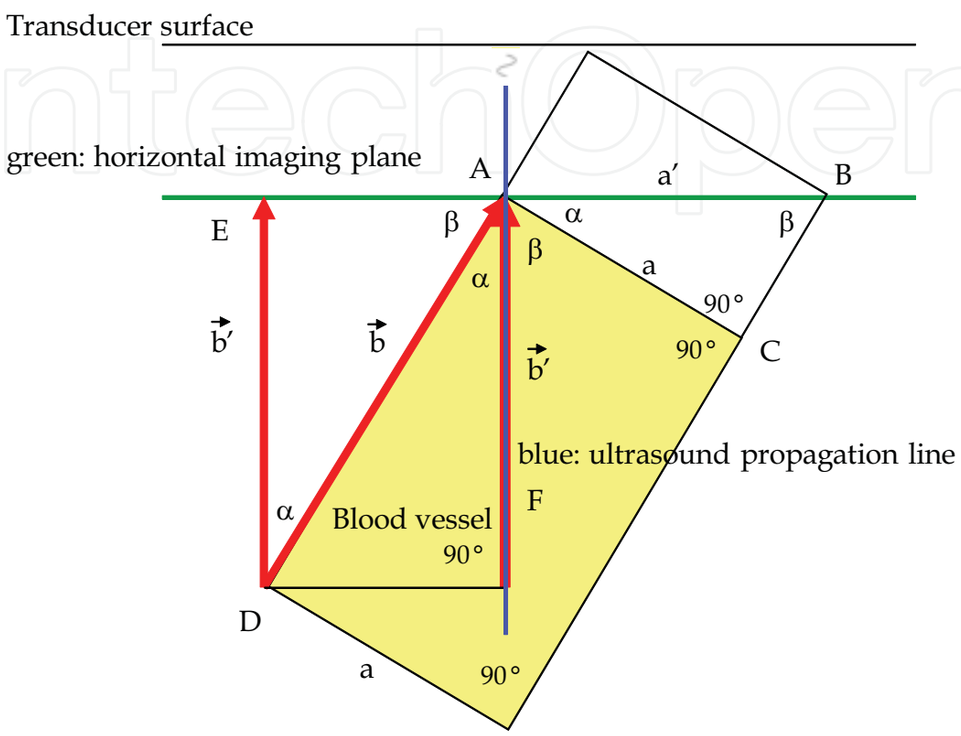

Fig. 30. Schematical depiction of a horizontally cut vessel in a 3D-color Doppler sonographic dataset

19. References

[1] Chameleon-Software, *PixelFlux*. 2011. http://www.chameleon-software.de/index-de.html.

[2] Scholbach T., DiMartino E., Scholbach J. "Dynamic color Doppler sonographic tissue perfusion measurement in tumors" in Cancer imaging (2 volumes) (Elsevier/ Academic Press, 2008) ed by M.A. Hayat

[3] Scholbach, T. and J. Scholbach, Can We Measure Renal Tissue Perfusion by Ultrasound? *Journal of Medical Ultrasound*, 2009. 17(1): p. 9-16.

[4] Wieczorek, A., et al., The assessment of normal female urethral vascularity with Color Doppler endovaginal ultrasonography: preliminary report. *Pelviperineology* 2009. 28: p. 59-61.

[5] Masulli, M., et al., Measurement of the intrarenal arterial resistance index for the identification and prediction of diabetic nephropathy. *Nutr Metab Cardiovasc Dis*, 2009. 19(5): p. 358-64.

[6] Radermacher, J., et al., The renal arterial resistance index and renal allograft survival. *N Engl JMed*, 2003. 349(2): p. 115-24.

[7] Ozelsancak, R., et al., Relationship between renal resistive index and inflammation in untreated hypertensive patients. *Int Heart J*, 2009. 50(6): p. 753-61.
[8] Crutchley, T.A., et al., Clinical utility of the resistive index in atherosclerotic renovascular disease. *JVasc Surg*, 2009. 49(1): p. 148-55, 155 e1-3; discussion 155.
[9] Soria Galvez, F., et al., [Usefulness of renal resistive index in the diagnosis and evolution of the obstructive uropathy. Experimental study]. *Actas Urol Esp*, 2007. 31(1): p. 38-42.
[10] Onur, M.R., et al., Role of resistive index in renal colic. *Urol Res*, 2007. 35(6): p. 307-12.
[11] Krumme, B. and M. Hollenbeck, Doppler sonography in renal artery stenosis--does the Resistive Index predict the success of intervention? *Nephrol Dial Transplant*, 2007. 22(3): p. 692-6.
[12] Braun, B., Focal liver processes: "better is the enemy of good": CEUS in the fast lane. *Ultraschall Med*, 2009. 30(4): p. 329-32.
[13] D'Onofrio, M., et al., Focal liver lesions: sinusoidal phase of CEUS. *Abdom Imaging*, 2006. 31(5): p. 529-36.
[14] Trojan, J., et al., Contrast-enhanced ultrasound in the diagnosis of malignant mesenchymal liver tumors. *JClin Ultrasound*. 38(5): p. 227-31.
[15] Dietrich, C.F., et al., Pitfalls and artefacts using contrast enhanced ultrasound. *Z Gastroenterol*. 49(3): p. 350-6.
[16] Hocke, M., et al., Contrast-enhanced endoscopic ultrasound in discrimination between benign and malignant mediastinal and abdominal lymph nodes. *J Cancer Res Clin* Oncol, 2008. 134(4): p. 473-80.
[17] O'Connor, P.M., Renal oxygen delivery: matching delivery to metabolic demand. *Clin Exp Pharmacol Physiol*, 2006. 33(10): p. 961-7.
[18] Wolff, C.B., Normal cardiac output, oxygen delivery and oxygen extraction. *Adv Exp Med Biol*, 2007. 599: p. 169 - 82.
[19] Ikee, R., et al., Correlation between the resistive index by Doppler ultrasound and kidney function and histology. *Am JKidney Dis*, 2005. 46(4): p. 603-9.
[20] Scholbach, T., I. Dimos, and J. Scholbach, A new method of color Doppler perfusion measurement via dynamic sonographic signal quantification in renal parenchyma. *Nephron Physiol*, 2004. 96(4): p. p99-104.
[21] Scholbach, T., From the nutcracker-phenomenon of the left renal vein to the midline congestion syndrome as a cause of migraine, headache, back and abdominal pain and functional disorders of pelvic organs. *Med Hypotheses*, 2007. 68(6): p. 1318-27.
[22] Scholbach, T., et al., Correlation of histopathology and dynamic tissue perfusion measurement (DTPM) in renal transplants. http://www.postersessiononline.com/173580348_eu/congresos/48era/aula/poster_43104.pdf, 2011(ERA-EDTA Congress 2011).
[23] Scholbach, T., E. Girelli, and J. Scholbach, Dynamic tissue perfusion measurement: a novel tool in follow-up of renal transplants. *Transplantation*, 2005. 79(12): p. 1711-6.
[24] Scholbach, T., E. Girelli, and J. Scholbach, Tissue pulsatility index: a new parameter to evaluate renal transplant perfusion. *Transplantatio*n, 2006. 81(5): p. 751-5.
[25] Marti, E., et al., Donor effect on cortical perfusion intensity in renal allograft recipients: a paired kidney analysis. *Am JNephrol*. 33(6): p. 530-6.
[26] Scholbach, T., I. Herrero, and J. Scholbach, Dynamic color Doppler sonography of intestinal wall in patients with Crohn disease compared with healthy subjects. *JPediatr Gastroenterol Nutr*, 2004. 39(5): p. 524-8.

[27] Scholbach, T., J. Hormann, and J. Scholbach, Dynamic tissue perfusion measurement of the intestinal wall - correlation to histology in ulcerative colitis. *Journal of Medical Ultrasound* 2010. 18(2): p. 62-70.

[28] Cassia, G., et al., Hypoxic ischemic injury: intestinal appearances and perfusion measurements using ultrasound and dynamic color Doppler sonography in neonates submitted to therapeutic hypothermia. *Pediatr Radiol*, 2011. 41(Suppl 1): p. S250-S310 FN-9.

[29] Schäfer, M., Dynamische farbduplexsonografische Gewebeperfusionsmessung an cervicalen Lymphknoten (Dissertationsschrift). Katalog der Deutschen Nationalbibliothek, 2009: p. http://d-nb.info/1002591465

[30] Oktar, S., et al., Quantitative Color Doppler Evaluation of Perfusion in the Differential Diagnosis of Benign and Malignant Thyroid Nodules Using a Dedicated Software Program.
http://rsna2007.rsna.org/rsna2007/v2007/conference/event_display.cfm?am_id=3&em_id=5008569, 2007.

[31] Vaupel, P., et al., Hypoxia in breast cancer: role of blood flow, oxygen diffusion distances, and anemia in the development of oxygen depletion. *Adv Exp Med Biol*, 2005. 566: p. 333-42.

[32] Vaupel, P. and A. Mayer, Hypoxia and anemia: effects on tumor biology and treatment resistance. *Transfus Clin Biol*, 2005. 12(1): p. 5-10.

[33] Vaupel, P., Prognostic potential of the pre-therapeutic tumor oxygenation status. *Adv Exp Med Biol*, 2009. 645: p. 241-6.

[34] Scholbach, T., et al., New method of dynamic color doppler signal quantification in metastatic lymph nodes compared to direct polarographic measurements of tissue oxygenation. *Int JCancer*, 2005. 114(6): p. 957-62.

[35] Ebrashy, A., et al., Middle cerebral/umbilical artery resistance index ratio as sensitive parameter for fetal well-being and neonatal outcome in patients with preeclampsia: case-control study. *Croat Med J*, 2005. 46(5): p. 821-5.

[36] Figueras, F., et al., Umbilical artery pulsatility index: reliability at different sampling sites. *JPerinat Med*, 2006. 34(5): p. 409-13.

[37] Eik-Nes, S.H., K. Marsal, and K. Kristoffersen, Methodology and basic problems related to blood flow studies in the human fetus. *Ultrasound Med Biol*, 1984. 10(3): p. 329-37.

[38] Gill, R.W., et al., Umbilical venous flow in normal and complicated pregnancy. *Ultrasound Med Biol*, 1984. 10(3): p. 349-63.

[39] Erskine, R.L. and J.W. Ritchie, Quantitative measurement of fetal blood flow using Doppler ultrasound. *Br JObstet Gynaecol*, 1985. 92(6): p. 600-4.

[40] Scholbach T., Stolle J., Scholbach J. Three dimensional volumetric spatially angle corrected pixelwise fetal flow volume measurement. *Eur J Ultrasound* (2011 accepted for publication)

[41] Herzog, K., et al., Luteal blood flow is a more appropriate indicator for luteal function during the bovine estrous cycle than luteal size. *Theriogenology*. 73(5): p. 691-7.

[42] Luttgenau, J., et al., Low plasma progesterone concentrations are accompanied by reduced luteal blood flow and increased size of the dominant follicle in dairy cows. *Theriogenology*. 76(1): p. 12-22.

[43] Bollwein, H., et al., Effects of a shortened preovulatory follicular phase on genital blood flow and endometrial hormone receptor concentrations in Holstein-Friesian cows. *Theriogenology*. 73(2): p. 242-9.
[44] Beindorff, N., et al., Effects of human chorionic gonadotropin on luteal blood flow and progesterone secretion in cows and in vitro-microdialyzed corpora lutea. *Theriogenology*, 2009. 72(4): p. 528-34.
[45] Herzog, K., et al., Luteal blood flow increases during the first three weeks of pregnancy in lactating dairy cows. *Theriogenology*. 75(3): p. 549-54.
[46] Luttgenau, J., et al., Plasma progesterone concentrations in the mid-luteal phase are dependent on luteal size, but independent of luteal blood flow and gene expression in lactating dairy cows. *Anim Reprod Sci*. 125(1-4): p. 20-9.
[47] Pancarcı, Ş.M., et al., Changes in follicular blood flow and nitric oxide levels in follicular fluid during follicular deviation in cows. *Animal Reproduction Science*, 2011. 123 (3-4): p. 149-156.
[48] Kuchler, K., et al., Measuring the blood flow of teats of dairy cows by using Color-Angiography. *Reproduction in Domestic Animals*, 2011. 46(S1): p. 25 http://onlinelibrary.wiley.com/doi/10.1111/j.1439-0531.2011.01755.x/pdf.
[49] Rouviere, O., et al., Can color doppler predict the uniformity of HIFU-induced prostate tissue destruction? *Prostate*. 2004 60(4): p. 289-97.
[50] Aslan, M., et al., Quantitative Analysis of Ultrasonographic Textures with Software in Experimental Testicular Torsion. *Turkish Association of Pediatric Surgeons*, 2011. http://www.tccd.org.tr/abstract/yayinlanan_bildiri.php?bid=77.
[51] Faingold, R., et al., Cerebral perfusion measurements using dynamic color Doppler sonography in neonates with hypoxic ischemic encephalopathy (HIE) treated with therapeutic hypothermia. *Pediatr Radiol* 2011. 41(Suppl 1): p. S250-S310 NE2-3.

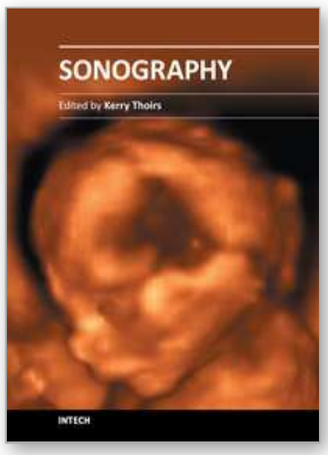

Sonography

Edited by Dr. Kerry Thoirs

ISBN 978-953-307-947-9
Hard cover, 346 pages
Publisher InTech
Published online 03, February, 2012
Published in print edition February, 2012

Medical sonography is a medical imaging modality used across many medical disciplines. Its use is growing, probably due to its relative low cost and easy accessibility. There are now many high quality ultrasound imaging systems available that are easily transportable, making it a diagnostic tool amenable for bedside and office scanning. This book includes applications of sonography that can be used across a number of medical disciplines including radiology, thoracic medicine, urology, rheumatology, obstetrics and fetal medicine and neurology. The book revisits established applications in medical sonography such as biliary, testicular and breast sonography and sonography in early pregnancy, and also outlines some interesting new and advanced applications of sonography.

INTECH
open science | open minds

InTech Europe
University Campus STeP Ri
Slavka Krautzeka 83/A
51000 Rijeka, Croatia
Phone: +385 (51) 770 447
Fax: +385 (51) 686 166
www.intechopen.com

InTech China
Unit 405, Office Block, Hotel Equatorial Shanghai
No.65, Yan An Road (West), Shanghai, 200040, China
中国上海市延安西路65号上海国际贵都大饭店办公楼405单元
Phone: +86-21-62489820
Fax: +86-21-62489821

IntechOpen